Syu *et al.*
Terrestrial, Atmospheric and Oceanic Sciences (2025) 36:22
https://doi.org/10.1007/s44195-025-00096-8

Terrestrial, Atmospheric and Oceanic Sciences

ORIGINAL ARTICLE Open Access

Characterization of carbon storage systems in central Taiwan and its offshore area

Wei-Di Syu[1], Andrew Tien-Shun Lin[1,2*], Chi-Wen Yu[3], Jia-Jyun Dong[1], Ming-Wei Yang[4], Chung Huang[4] and Shu-Kun Hsu[1]

Abstract

Geological carbon storage is widely used to reduce CO_2 emissions to the atmosphere. Cenozoic rock strata up to 8 km in thickness, consisting of thick sandstone and shale layers in central Taiwan and offshore areas, where major emitting sources are located, are investigated for their carbon storage potential. Four carbon storage systems are characterized in the aspects including the spatial distribution of lithologies, formation thicknesses, depths, permeability, and porosity of the reservoirs, using data from 22 boreholes and a few seismic sections. Three sites, the Taichung Power Plant (TPP), Changhua Coastal Industrial Park (CCIP), and Mailiao Taisu Industrial Park (MTIP), are selected for detailed site characterization. The storage systems, each composed of a caprock and reservoir pair, are (1) R1 system of the lower Cholan Formation (Fm); (2) R2 system from the Chinshui Shale (Sh), Kueichulin Fm, to Nanchuang Fm, and Kuanyinshan Sandstone (Ss); (3) R3 system from the Talu Sh to Peiliao Fm and Shihti Fm; and (4) R4 system from the Piling Sh to Mushan Fm and Wuchishan Fm. The four systems above show spatial depth variations and lateral changes in the lithofacies of caprocks and reservoirs, leading to different storage systems from site to site. Our results indicate that central Taiwan and offshore areas are ideal for the geological sequestration of CO_2 and that their capacity to host CO_2 requires further investigation.

Highlights

- Four carbon storage systems in central Taiwan and its offshore area are identified.
- Measured reservoir porosity and permeability values from borehole cores are presented.
- Storage potentials are discussed in detail at three coastal sites near major CO_2 emission sources.

Keywords Geological carbon storage, Caprock, Reservoir, Porosity, Permeability, Central Taiwan

1 Introduction

Carbon capture and storage (CCS) is widely used to mitigate atmospheric CO_2 emissions in the atmosphere (Anwar et al. 2018). The proposal of 'Net Zero Emission by 2050' under the Paris Agreement was adopted by 196 Parties at COP 21 in Paris on 12 December 2015 and entered into force on 4 November 2016 (Savaresi 2016). To achieve 'Net Zero Emission by 2050', the Taiwanese government intends to deploy CCS technology widely to reduce CO_2 emissions, with a goal of reducing 40.2 Mt of CO_2 annually by 2050 (NDC 2022). Therefore, an

*Correspondence:
Andrew Tien-Shun Lin
andrewl@ncu.edu.tw
[1] Department of Earth Sciences, National Central University, 300 Jungda Road, Chungli, Taoyuan 320317, Taiwan
[2] Carbon Storage and Geothermal Research Center, National Central University, Taoyuan, Taiwan
[3] Sinotech Engineering Consultants, Inc., Taipei City, Taiwan
[4] Taiwan Power Company, Taipei City, Taiwan

assessment of carbon storage capacity and stratigraphic storage systems is essential for future CCS deployment in Taiwan.

In central–western Taiwan, the need for prompt investigations is pressing due to the prevalent infrastructure of large power plants and industrial parks that produce significant CO_2 emissions in the area. In this study, we used borehole data from 21 hydrocarbon exploration wells (Lin 2001; Lin et al. 2003, 2016; Lin et al. 2021a, b) and an additional borehole, TPCS-M1 (M1), to identify carbon storage systems and thier spatial variations in formation depth, thickness, and lithology in the study area. The criteria proposed by Chadwick et al. (2008) and Bachu et al. (2009) were adopted, including fundamental rock pair of reservoir and seal, minimum burial depth (> 800 m), layer thickness (≧10–20 m), porosity (≧10%), and permeability (≧20 mD). The carbon storage systems are specifically evaluated at three sites with massive emissions of great concern: the Taichung Power Plant (TPP), Changhua Coastal Industrial Park (CCIP), and Mailiao Taisu Industrial Park (MTIP).

2 Geological setting and stratigraphy

The study area (Fig. 1), central Taiwan, and the offshore area lie in the central-southern Taihsi Basin (TB). The TB is an early Paleogene rift basin overlain by Oligocene–Miocene post-breakup sediments and the overlying late Miocene-Recent foreland-basin succession (Lin et al. 2003). The passive-margin successions deepen toward the east because of the flexure of the Taiwan mountain belt (Lin and Watts 2002) in addition to the thermal cooling and deepening toward the distal margin in the east during the Oligocene to late Miocene. The TB is bounded to the north by the Kuanyin Platform and the Penghu Platform (PHP) to the south. Peikang High (PKH) is located at the eastern edge of the PHP. Cenozoic sediments up to 8 km thick, consisting of thick sandstone and shale layers, in the TB provide multiple carbon storage systems.

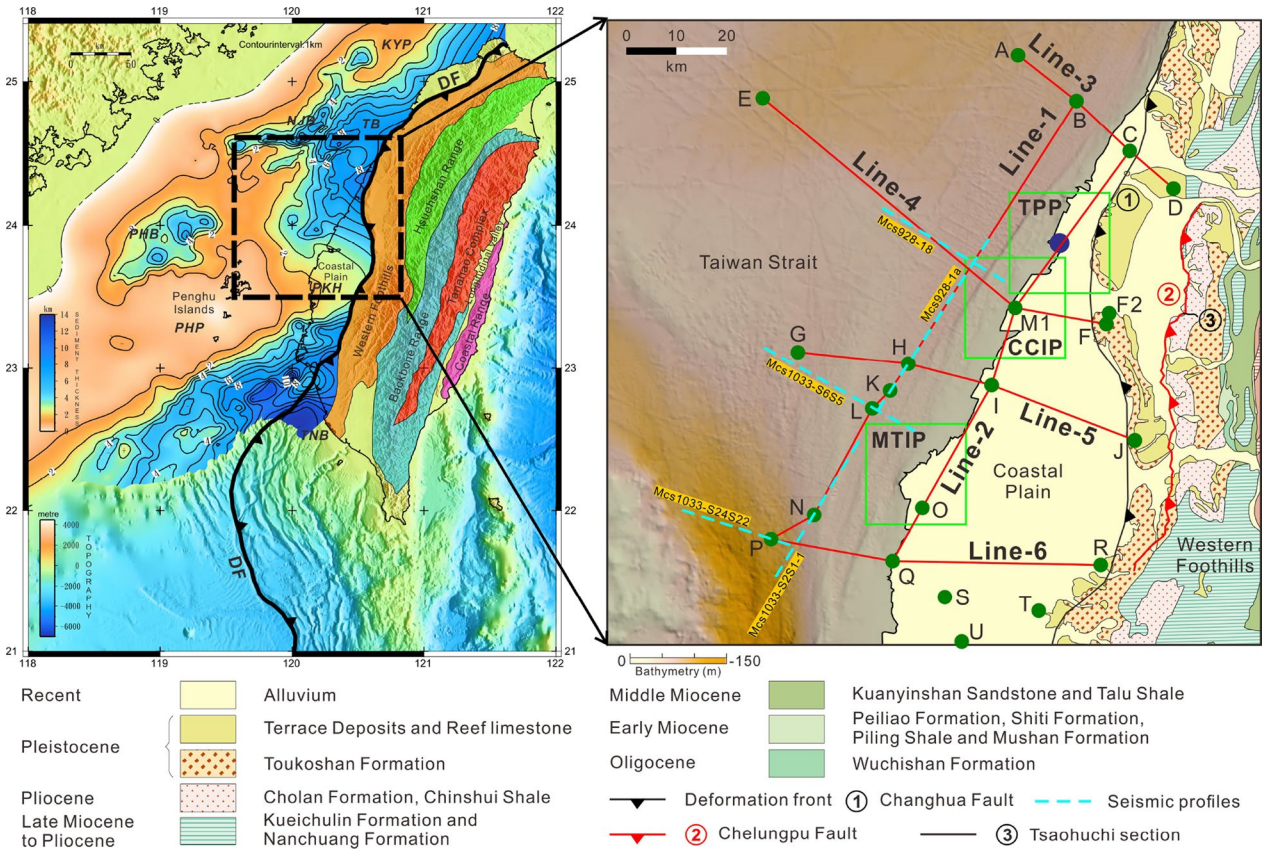

Fig. 1 **a** Topographic and bathymetric features in Taiwan with color-coded contour depth map (in km) showing the top of the Mesozoic basement (Mesozoic basement from Lin et al 2003) and major geo-tectonic units in the Taiwan island. The thick, barbed black line indicates the frontal compressive structure. **b** Geological map in western-central Taiwan (Central Geological Survey 1986) and bathymetry in the eastern Taiwan Strait. Locations and names of studied boreholes (green dots), borehole correlation panels (red lines), three sites (TPP, CCIP, MTIP sites marked in green rectangles), Taichung Power Plant (blue dots), and Tsaohuchi section (black line with circle no.3) for detailed discussion are also shown. Acronyms for the tectonic unit (Lin et al. 2003) are *KYP* Kuanyin Platform, *NJB* Nanjihtao Basin, *PHB* Penghu Basin, *PHP* Penghu Platform, *PKH* Peikang High (Hu et al. 1997), *TNB* Tainan Basin, and *TB* Taihsi Basin

Depending on the geological units, central Taiwan is divided into the western foothills of the Taiwan mountain belt, the coastal plain, and the eastern Taiwan Strait. The western foothills comprise a series of active thrust-and-fold belts, with the Changhua fault and a related anticline (Pakua anticline) as frontal compressive structures. The coastal plain and the eastern Taiwan Strait pertain to the foreland basin (Lin and Watts 2002; Lin et al. 2003), with formations dipping gently toward western foothills.

The study area has experienced basin developments from the Paleocene–Eocene syn-rift episode (~58–37 Ma), the post-breakup episode (~30–6.5 Ma), and the foreland and orogenic belt episode (6.5 Ma to present; Lin et al. 2003; Teng and Lin 2004). The deposits that accumulated during the post-breakup episode (approximately 30–6.5 Ma) in the passive continental margin are, in ascending order, Wuchishan Fm, Mushan Fm, Piling Sh, Shiti Fm, Peiliao Fm, Talu Shale (Sh), Kuanyinshan Sandstone (Ss), and Nanchuang Fm (Fig. 2). The stratigraphy description of the Wuchishan Fm to the Nanchuang Fm is shown in Figs. 3 and 4. Formations in the foreland basin (6.5 Ma to present) include, from bottom to top, the Kueichulin Fm, Chinshui Sh, Cholan Fm, and Toukoshan Fm (Fig. 2). The stratigraphy description of the Kueichulin Fm to the Toukoshan Fm is shown in Fig. 5.

The Paleogene sediments are not considered good CO_2 storage systems for the following reasons: (1) Their depth is mostly over 3500 m and thus limited storage potential. The porosity and permeability of the Paleogene sediments are also poor (Lin et al. 2003). (2) Even if the Paleogene sediments are located within suitable depth ranges, existing boreholes (e.g. E, G, H, I, K, L, N, O, P, and Q) indicated that the Paleogene sediments are composed mostly of shale and tuff with thin sandstone beds (Chan et al. 1978; Chang et al. 1978; Ye et al. 1993).

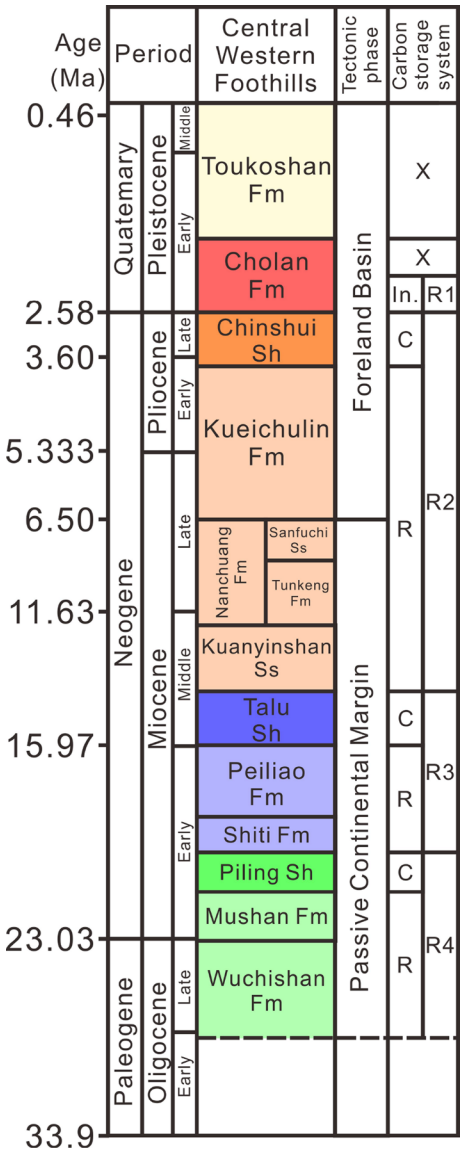

Fig. 2 Stratigraphy and proposed carbon storage systems in central Taiwan. Eleven formations are divided into four storage systems: R1, R2, R3, and R4. R1 system: Lower Cholan Fm; R2 system: Chinshui Sh, Kueichulin Fm, Nanchuang Fm, and Kuanyinshan Ss. Nanchuang Fm is further divided into Sanfuchi Ss and Tunkeng Fm; R3 system: Talu Sh, Peiliao Fm, and Shiti Fm; R4 system: Piling Sh, Mushan Fm, and Wuchishan Fm. The formations in storage systems are further divided as cap rock (labeled as C), reservoir rocks (R), and interbedded sandstones and shale (In)

3 Data and carbon storage system

3.1 Borehole data and seismic profile

We collected 22 well data down to 1300 to 5200 in depth, from nine onshore boreholes and thirteen offshore ones. Twenty-one of them are hydrocarbon exploration wells drilled by the CPC Corporation, Taiwan, and have been reported by Lin (2001), Lin et al. (2003), Yu et al. (2013), Lin et al. (2016), and Lin et al. (2021a; b). The M1 well is drilled by the Taiwan Power Company at the CCIP for carbon storage. Some CPC borehole data can be found in the project report of Lin et al. (2016), which is a joint project between the Ministry of Science and Technology, the CPC Corporation, and the Taiwan Power Company. The drilled depths of the studied boreholes are in the range of 1300–5200 m. The studied 22 boreholes are evenly distributed in the study area with good spatial coverage, which is therefore considered sufficient for characterizing the carbon storage systems in central Taiwan.

The 18 boreholes had collected logs of the spontaneous potential (SP), gamma ray (GR), sonic log (DT), and resistivity (including ILD and RLA). The logs, together with the description of well cuttings, were used to determine the lithology and formation depths and therefore, the

Example stratigraphy (Borehole I)	Formation and age	Depositional environment, lithology and geometry
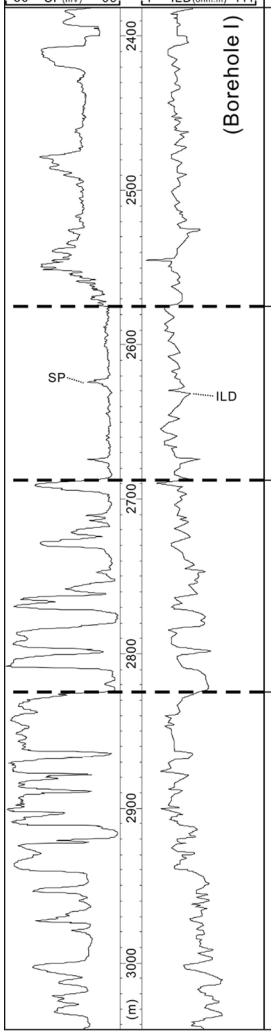	Shiti Fm early Miocene ~19.9–19 Ma	The Shiti Fm was deposited in coastal to shelf environments (Chou, 1976). The lithology comprises fine- to medium-grained quartz sandstones alternating with thin shale beds, including several coal seams in northern Taiwan. The formation thickness is around 650 m in the proximal coastal setting in the north of the study area, and it decreases southwardly to around 200 m in the distal shelf setting in the south (Lin et al., 2021a).
	Piling Sh early Miocene ~21–19.9 Ma	The Piling Sh was deposited in inner to outer shelf environments. The lithology comprises thick shale, siltstone, and thin sandstone. The middle part of the Piling Sh has a ten-meter-thick sandstone layer. The thickness is around 400 m in the north of the study area, decreasing to around 150 m in the south (Lin et al., 2021a).
	Mushan Fm early Miocene ~23.9–21 Ma	The Mushan Fm was deposited in fluvial to coastal environments (Hsieh, 1968). The lithology comprises interbedded sandstone/shale and thick medium-grained quartz sandstones with thin coal seams in northern Taiwan. The thickness is around 600 m in the north of the study area (Hsieh, 1968), decreasing southward, and pinches out at the Peikang High (Lin et al., 2021a).
	Wuchishan Fm late Oligocene ~27.5–23.9 Ma	The Wuchishan Fm was deposited in coastal and shallow-marine environments (Chou, 1974; Lin et al., 2021a). The lithology comprises medium- to coarse-grained quartz sandstone alternating with thick shale beds. The thickness is around 300 m in the north of the study area. It decreases southward to 200 m thick at the borehole PKS-2 (Chou, 1974) and pinches out at Peikang High (Lin et al., 2021a).

Fig. 3 Description of stratigraphy for the Wuchishan Fm, Mushan Fm, Piling Sh, and Shiti Fm. Logs of borehole I is used to demonstrate example vertical lithologic variations

carbon storage system. The spatial distribution of each carbon storage system is shown in six borehole correlation panels (Fig. 1).

We also collected porosity and permeability data from previous studies, where the values were measured from core samples from nine boreholes. The data sources are listed below. The porosity and permeability data from the M1 well were previously reported in Sinotech Engineering Consultants, Inc. (2014), Yang (2015), and Lin (2018). The porosity and permeability values of R2 systems were reported in Hsu et al., (1969), Yang et al. (1969), and Yang et al. (1971); R3 system, in Yang et al. (1971), Chan et al. (1974), and Hsieh et al. (1974); and R4 system, in Hsieh, (1962), Hsu et al. (1969), Yang et al. (1969), Chan et al. (1978), and Wu et al. (1991). The porosity and permeability values for M1 well as reported by Yang (2015) and Lin (2018), were measured under various effective confining pressures, and they also employed a stress history-dependent model (Wu and Dong 2012) to estimate the porosity and permeability values under atmospheric pressure. The porosity and permeability values from M1 well as reported by Sinotech Engineering Consultants, Inc. (2014), and other boreholes were measured under atmospheric pressure.

We correlated the formation boundaries from the boreholes to five offshore seismic profiles to show the spatial variations in the studied formations. The locations of these five seismic sections are shown in Fig. 1.

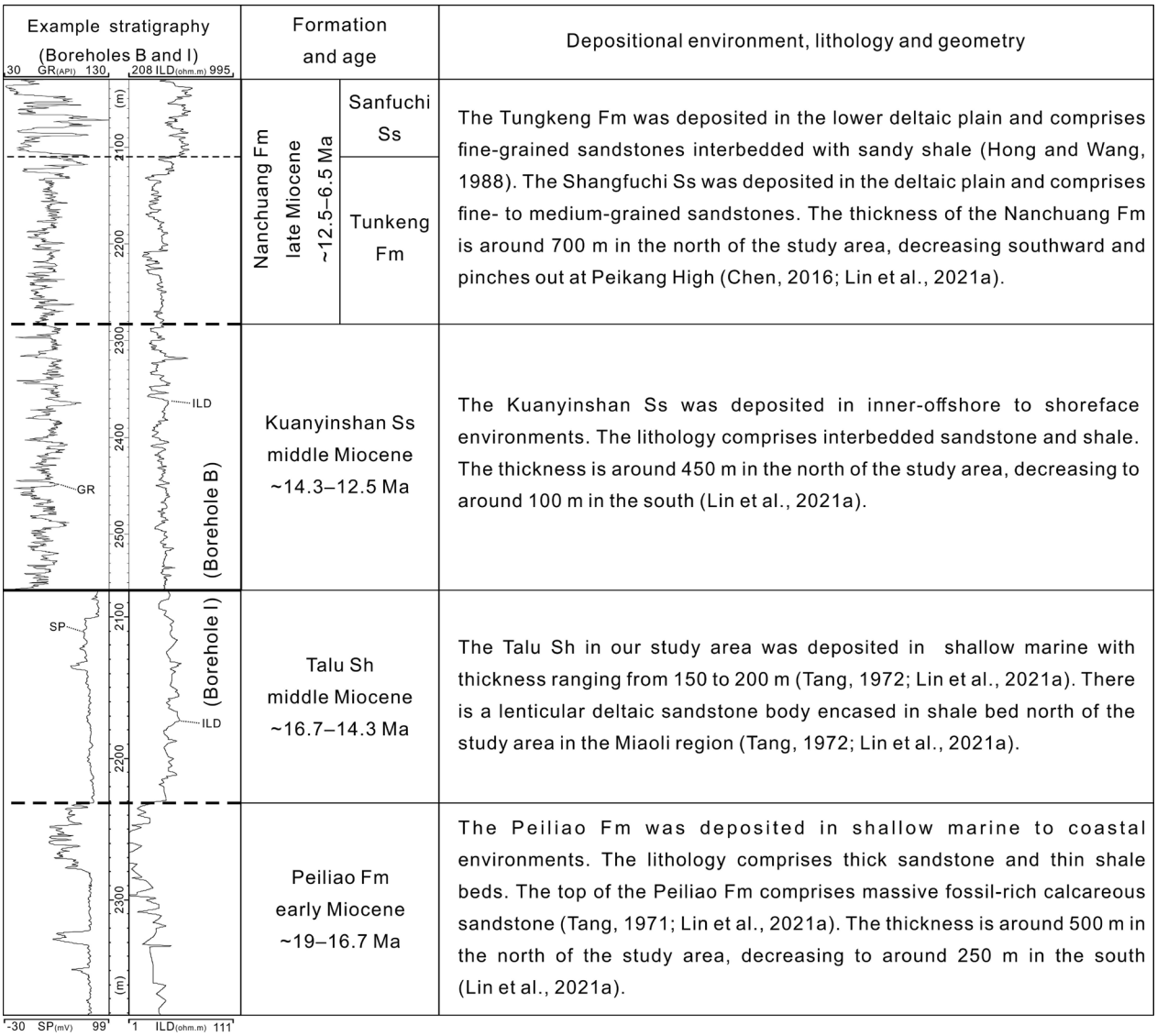

Fig. 4 Description of stratigraphy for the Peiliao Fm, Talu Sh, Kuanyinshan Ss, and the Nanchuang Fm. Logs of boreholes B and I are used to demonstrate example vertical lithologic variations

The seismic profiles were collected by onboard research vessels by the research projects of Hsu et al. (2013) and Lin et al. (2014) for MCS928 and MCS1033 seismic lines, respectively.

3.2 Carbon storage systems

An ideal carbon storage system should consist of coupled high-capacity reservoir rock and impermeable seal rock (Chadwick et al. 2008; Bachu et al. 2009) at depths greater than 800 m, where the injected CO_2 maintains a supercritical phase (Sasaki et al. 2008; Brantley et al. 2015; Ma and He 2017). The lower depth limit of the injected CO_2 depends on the CO_2 injectivity (i.e., rock porosity and permeability) and compression energy consumption during injection, which is a function of the formation pressure. Lin (2008) estimated that a 3000 m depth corresponds to the maximum CO_2 trapping capacity in terms of residual gas and solubility trapping and a 1300 m depth represents the maximum net financial income. The amount of CO_2 produced due to the consumption of energy for CO_2 storage per unit mass is around 15% of stored CO_2, even when the CO_2 is injected at a depth of 7000 m (Lin 2008). According to Lin et al. (2003), porosity is less than 10% in the Cenozoic deposits below 3500 m in depth in Taiwan, which marks the maximum efficient depth in this study. The minimum efficient

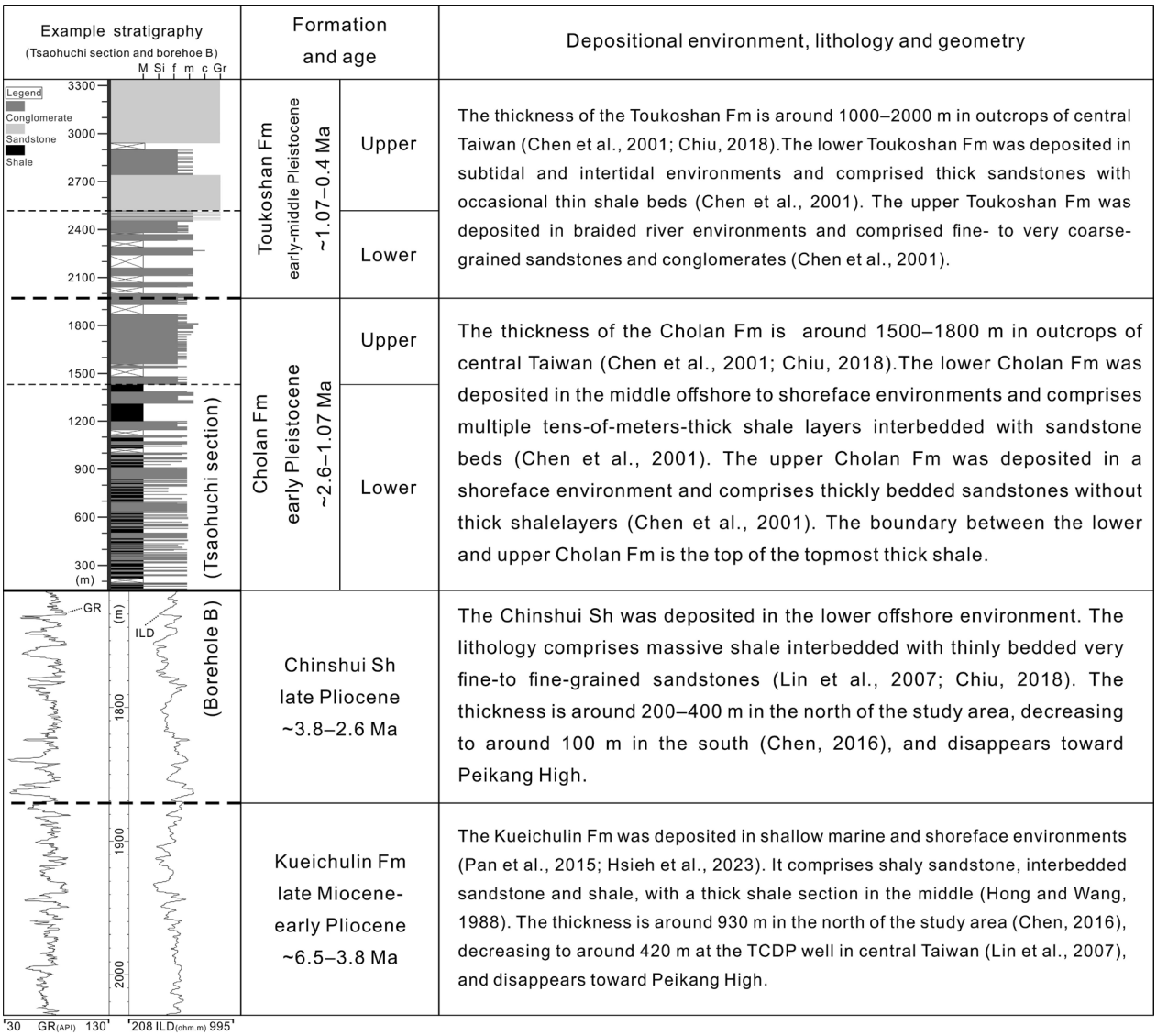

Fig. 5 Description of stratigraphy for the Kueichulin Fm, Chinshui Sh, Cholan Fm, and the Toukoshan Fm. Logs of borehole B and the stratigraphic column of the Tsaohuchi outcrop section (Chen et al. 2001) are used to demonstrate example vertical lithologic variations

depth is set at 800 m, because CO_2 is unstable and out of a dense supercritical phase due to the rock temperature and pressure (Span et al. 1996; Ma and He 2017).

The regional shale layer is defined as the top of the carbon storage system. In central Taiwan, the rock formations of the Chinshui Sh, Talu Sh, and Piling Sh are thick shaly formations (> 100 m thick). Below the top shale of the storage system, various thick sandstone layers are present, which may serve as good CO_2 reservoirs. We assigned Chinshui Sh, Talu Sh, and Piling Sh as the top seals for carbon storage systems R2, R3, and R4, respectively. The R1 system is different from the other storage systems because it lacks a thick regional top shale layer. The lower part of the Cholan Fm consists of thick sandstone and shale beds of offshore to shoreface facies, with a thickness of approximately 1250 m. In contrast, the upper part consists of thickly bedded shoreface sandstones without thick shale beds and has a thickness of about 550 m. The boundary between the lower and upper Cholan Fm is the top of the topmost thick shale. Therefore, we defined the multiple interbedded shale layers as seals and the interbedded thick sandstones as reservoirs. The R1 system comprises multiple sub-storage systems. Depending on the aforementioned criteria, we divided the formations of the TB (Lin et al. 2003, TB in Fig. 1) into four carbon storage systems, including 11

formations, from top to bottom as follows (Figs. 2 and 6): (1) R1 system is the lower Cholan Fm; (2) R2 system is from the Chinshui Sh, Kueichulin Fm to Nanchuang Fm, and Kuanyinshan Ss; (3) R3 system is from the Talu Sh to Peiliao Fm and Shiti Fm; and (4) R4 system is from the Piling Sh to Mushan Fm and Wuchishan Fm. The caprock and reservoir of all the systems are shown in Fig. 2. We have divided the gross lithology in detail using well logs; therefore, the reservoirs are subdivided into several substorage systems. Figure 6 shows the four storage systems from the representative boreholes and outcrops. The R1 system is shown in the Tsaohuchi outcrop section (Chen et al. 2001), and systems R2, R3, and R4 are shown in boreholes B, O, and I, respectively.

4 Spatial distribution of carbon storage systems

Herein, we use six borehole correlation panels to demonstrate the spatial distribution of carbon storage systems in the study area (Table 1). The Line-1 and Line-2 correlation panels are offshore and run roughly parallel to the coastline, respectively (Figs. 7 and 8). The horizontal distance is scaled with the exact borehole locations shown in the panel, except for boreholes N, H, and L. They are adjacent to boreholes P and K, and the three dashed arrows on Line-1 show their exact location. Solid arrows along the correlation panels indicate the projected locations and distances of the centers of the potential carbon storage sites (TPP, CCIP, and MTIP). Lines 3–6 are oriented roughly east-to-west (Figs. 9, 10, 11 and 12) and arranged from north to south, showing the stratigraphic correlations of three to four boreholes, respectively.

4.1 R1 system

The R1 system is the lower Cholan Fm of the early Pleistocene. The Tsaohuchi outcrop section exemplifies this system (Fig. 6), and Chen et al. (2001) describe the lithology, with its location shown in Fig. 1. The upper Cholan Fm and Toukoshan Fm are unsuitable for carbon storage because they do not contain thick shale to seal the stored CO_2. The upper section of R1 consists mainly of several layers of sandstone and shale, each of which is over 40 m thick. The lower section comprises multiple layers of sandstone and mudstone, with individual bed thicknesses that can reach up to 50 m. Bachu et al. (2009) propose that several layers of shale, each several tens of meters thick, may serve as efficient seal rock. Therefore, we defined thick sandstone beds as reservoirs and multiple thick shale layers as caprocks in the R1 system. However, the lower Cholan Fm grades into sandy deposits in the west (e.g., Figs. 9, 10, 11 and 12), where the intraformational sealing capacity decreases. Approximately six groups of substorage systems are present in the Tsaohuchi outcrop section (Fig. 6). We also have correlated the stratigraphic column of the Tsaohuchi outcrop section (Chen et al. 2001) with nearby boreholes, as shown in Line-4 (Fig. 10), to visualize the lateral lithological variations of the R1 system.

Overall, the top and basal depths of the R1 system range from 485 to 2935 m (top) and from 485 to 3690 m (base). The R1 system is the thickest and deepest in the NE, becoming the thinnest and shallowest toward the southwest. R1 system becomes sandy to the south and west. Therefore, the R1 system is a good carbon storage system in the NE and poor in the west and south of the study area regarding depth distribution and seal/reservoir-rock pairs.

For the north-to-south correlation panels, as shown in Line-1 and Line-2 (Figs. 7 and 8), the R1 system is further divided into 4–5 subsystems with 10–40 m thick seal rocks and 10–80 m thick reservoirs. This system thins toward the south and disappears in borehole N (Fig. 7). South of the K and O wells (Figs. 7 and 8), part of the R1 system is shallower than 800 m. For the west-to-east correlation panels, as shown in Lines 3–6 (Figs. 9, 10, 11 and 12), the R1 system consisted of 2–6 subsystems with 10–150 m thick reservoirs and 10–70 m thick caprocks. Part of the R1 system is shallower than 800 m; it thins toward the west and disappears in boreholes E, G, and P (Figs. 10, 11 and 12).

4.2 R2 system

The R2 reservoirs comprise thick sandstone beds of the Kueichulin Fm, Nanchuang Fm, and Kuanyinshan Ss, with the Chinshui Sh serving as the regional caprock. Borehole B (Fig. 6) represents the vertical lithological variations in the R2 system in the offshore central TB (Fig. 1). The R2 system dates from the middle Miocene to the Pliocene (Fig. 2).

Overall, the R2 system features sandstone beds up to 600 m thick and caprock shale approximately 120 m thick, as illustrated in borehole B (Fig. 6). In this study, Chinshui Sh is approximately 120 m thick and has been informally divided into three units (Fig. 6). The upper and lower units are shale tens of meters thick. The middle unit comprises interbedded sandstone and shale beds.

The top reservoir comprises a sandstone layer from the Kueichulin Formation. In central Taiwan, the Kueichulin Formation is divided into three stratigraphic units, listed in ascending order: Kuantaoshan Ss, Shihliufen Sh, and Yutengping Ss (Hsieh et al. 2013, Fig. 6). The Kuantaoshan Ss comprises 40 m of thick sandstone. The Shihliufen Sh is a shale formation roughly 45 m thick. The Yutengping Ss comprises sandstones interspersed with a thin layer of shale (Fig. 6).

In central Taiwan, the Nanchuang Formation is split into the upper Sanfuchi Sandstone and the lower

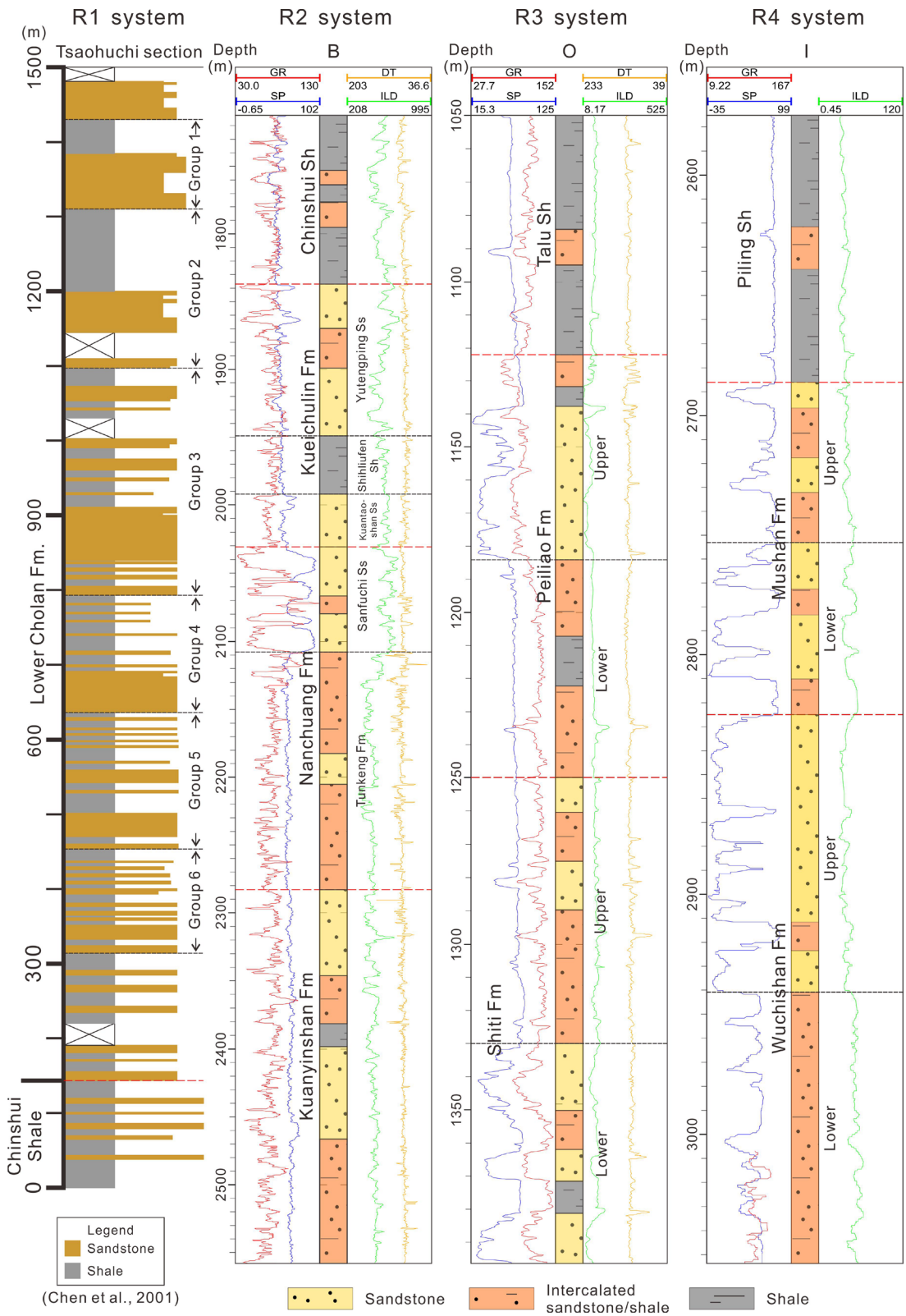

Fig. 6 Representative carbon storage systems with stratigraphic columns and well logs. The acronyms for well logs are DT: sonic log GR: gamma-ray log, ILD: induction resistivity log, and SP: spontaneous potential log. The R1 system is represented by the lower Cholan Formation exposed along the Tsaohu River (Tsaohuchi section), as reported in Chen et al. (2001). The R2, R3, and R4 systems are represented by the B, O, and I boreholes (see Fig. 1 for locations), respectively

Table 1 Depths, caprock thickness, and reservoir-rock thickness for systems from R1 to R4 along 6 borehole correlation panels (Line-1 to Line-6, see Fig. 1 for locations)

	Line-1	Line-2	Line-3	Line-4	Line-5	Line-6
Depth	485 – 1700 m	695 – 2415 m	830 – 2880 m	580 – 3500 m	490 – 3690 m	550 – 2480 m
R1 C. Thickness	10 – 20 m (4 – 5 layers)	10 – 40 m (3 – 6 layers)	10 – 50 m (3 – 6 layers)	10 – 70 m (5 layers)	10 – 70 m (5 layers)	10 – 60 m (2 – 4 layers)
R1 R. Thickness	10 – 30 m	10 – 80 m	15 – 80 m	10 – 105 m	10 – 150 m	10 – 100 m
Depth	370 – 2545 m	760 ~ 3465 m	1000 – 4035 m	170 – 3960 m	450 – 4000 m	370 – 2685 m
R2 C. Thickness	0 – 120 m	0 – 140 m	120 – 360 m	0 – 160 m	0 – 155 m	0 – 60 m
R2 R. Thickness	100 – 720 m	50 – 910 m	720 – 910 m	295 – 405 m	155 – 420 m	40 – 100 m
Depth	470 – 3680 m	795 – > 4000 m	2005 – > 4500 m	470 – 4520 m	875 – 4360 m	470 – 2940 m
R3 C. Thickness	95 – 560 m	75 – > 240 m	285 – 560 m	140 – 195 m	125 – 185 m	45 – 105 m
R3 R. Thickness	200 – 580 m	235 – > 345 m	495 – 580 m	380 – 395 m	195 – 405 m	205 – 230 m
Depth	785 ~ > 4000 m	1115 – > 4000 m	2995 – > 4000 m	995 – 5125 m	1325 – 4180 m	785 – 3055 m
R4 C. Thickness	70 – > 145 m	105 – > 120 m	~ 130 m	130 – 210 m	110 – 135 m	70 – 105 m
R4 R. Thickness	70 – > 605 m	0 – > 365 m	~ 710 m	140 – 395 m	365 – 605 m	25 – 75 m

C Caprocks, *R* Reservoir rocks

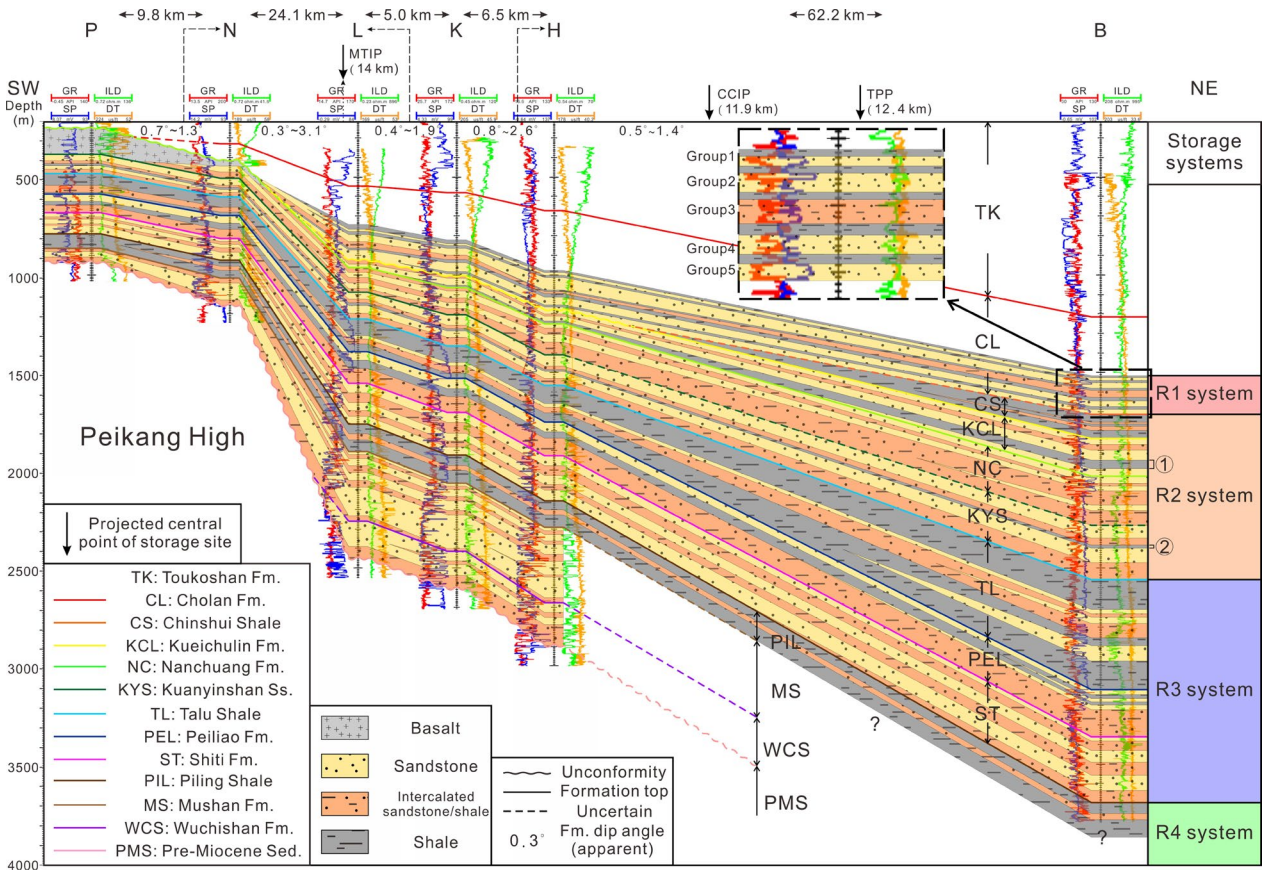

Fig. 7 Borehole stratigraphic correlation panel, Line-1, along the offshore NE-SW direction (see Fig. 1 for locations). Projected locations of studied sites (TPP, CCIP, MTIP) are also marked. Apparent formation dip angles along this profile and in-between boreholes are also labeled on the top. The Peikang High is PKH in Fig. 1

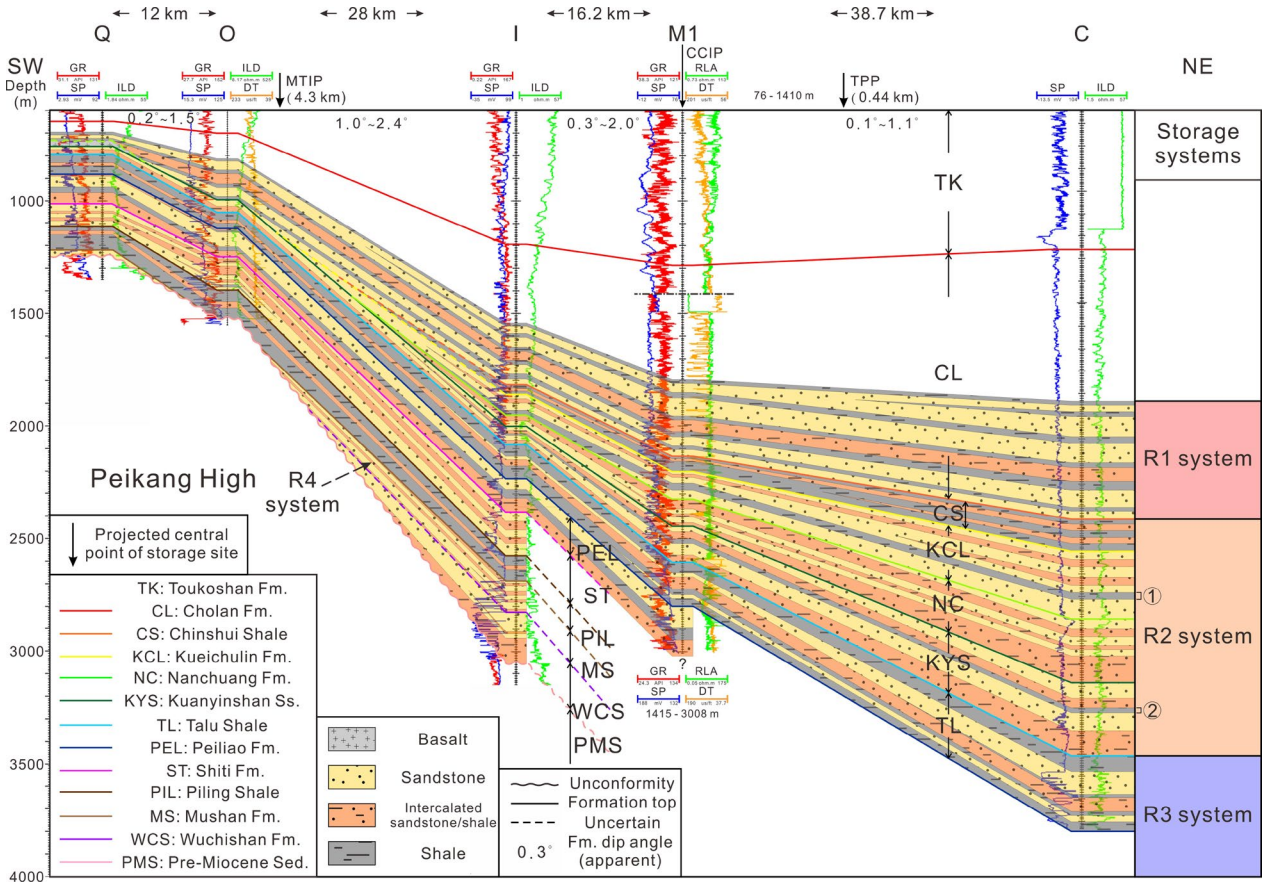

Fig. 8 Borehole stratigraphic correlation panel, Line-2, along the onshore NE-SW direction (see Fig. 1 for locations). Projected locations of studied sites (TPP, MTIP) are also marked, and the M1 well is in the middle of the CCIP site. Apparent formation dip angles along this profile and in-between boreholes are also labeled on the top. Acronyms for well logs are RLA: high-resolution array induction log. The Peikang High is PKH in Fig. 1

Tunkeng Formation (Figs. 2 and 6). The Sanfuchi Ss is approximately 90 m thick and consists of several meters of thick sandstone and a few thin shale layers. The Tunkeng Fm is approximately 170 m thick and comprises thickly bedded sandstone interspersed with shale beds (Fig. 6).

The bottom reservoir of the R2 system is the Kuanyinshan Ss, which is approximately 270 m thick (Fig. 6). The middle of the Kuanyinshan Ss has a thick shale of approximately 20 m, further dividing this stratigraphic unit into lower and upper sections. These sections primarily comprise thick sandstone beds.

According to the correlation panels, the R2 system in the NE area is suitable for CO_2 storage. However, in the south and west, it is too shallow and lacks a caprock, resulting in poor containment conditions. Regarding the north-to-south correlation panels illustrated in Line-1 and Line-2 (Figs. 7 and 8), the R2 system's top and basal depths vary from 370 to 2415 m (top) and from 470 to 3465 m (base), respectively. The regional seal, Chinshui Sh, is thick in the north at boreholes B and C (120–140 m thick), gradually thins toward the south, and disappears at boreholes H and O (Figs. 7 and 8). This indicates that the regional caprock for the R2 system is absent in the south of the study area. Underneath the Chinshui Sh caprock, the thickness of the remaining R2 reservoirs varies from 50 to 910 m (i.e., the cumulative thickness of the Kuichulin Fm, Nanchuang Fm, and Kuanyinshan Ss). The Kueichulin Fm and Kuanyinshan Ss include two thick and extensive shale layers that may serve as intraformational seals, similar to the concept proposed by Daniel and Kaldi (2008). The upper intraformational seal, located in the middle of the Kuichulin Fm (specifically, the Shihliufen Shale), can reach up to 40 m thick. However, it tapers off to the south and is absent in boreholes L and O (Figs. 7 and 8). The lower intraformational seal in the middle of the Kuanyinshan Ss is approximately 20 m thick. It is more widespread than the upper intraformational seal and appears in every borehole indicated in Line-1 (Fig. 7).

The west-to-east correlation panels (Figs. 9, 10, 11 and 12) show the R2 system features caprocks up to 360 m

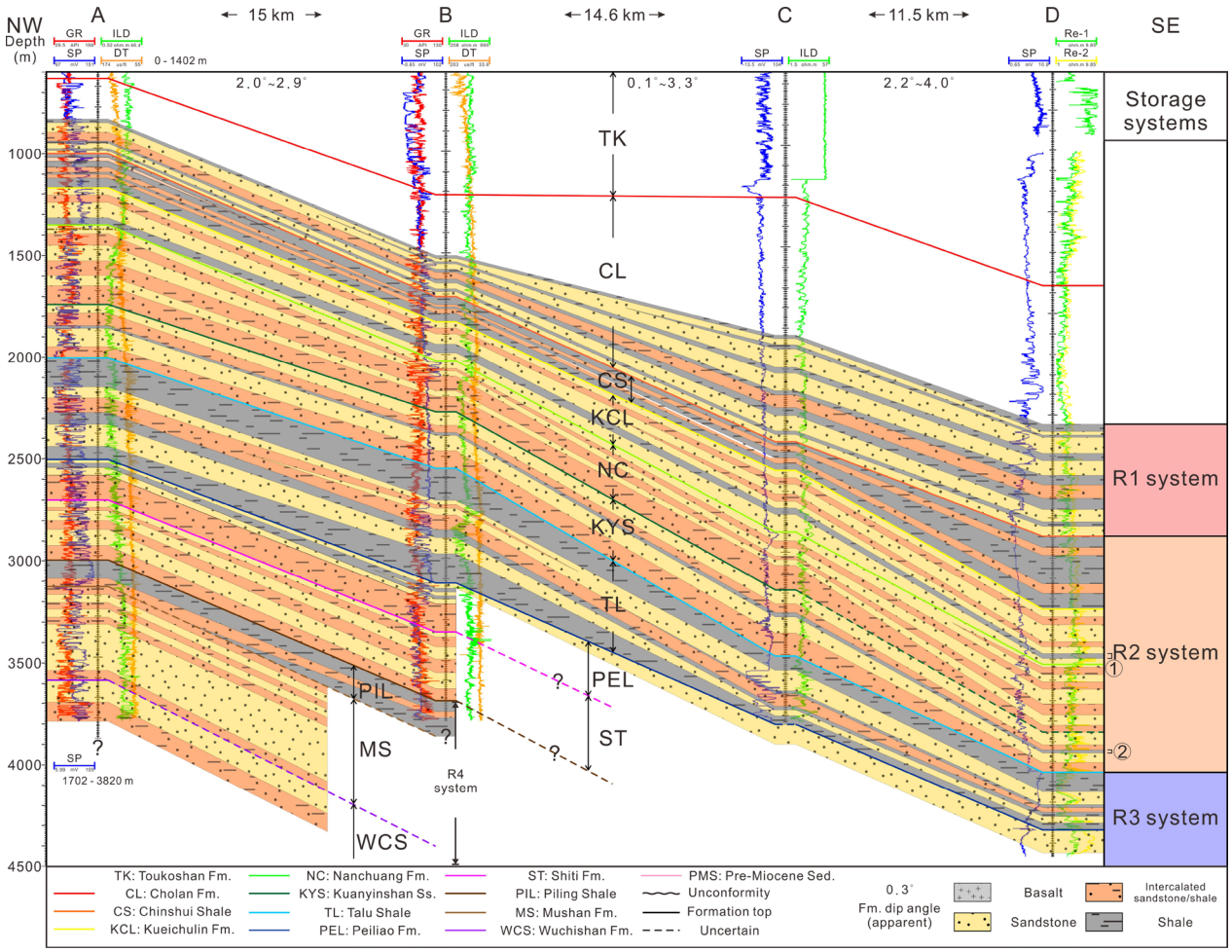

Fig. 9 Borehole stratigraphic correlation panel, Line-3, across the onshore and offshore NW–SE direction (see Fig. 1 for locations). Acronyms for well logs are Re-1 and Re-2: resistivity log

thick and reservoirs ranging from 40 to 910 m, with top depths from 170 to 3690 m and base depths from 470 to 4035 m. The Chinshui Sh thins toward the west and vanishes at several boreholes in the offshore area. The two intraformational seals are also displayed in the east–west correlation panels. The upper intraformational seal (Shihliufen Shale) is exclusively located in the northern region. In contrast, the lower intraformational seal within the Kuanyinshan Ss is more broadly distributed but notably absent in the southeastern area. However, the Nanchuang Fm is absent near borehole O and is substituted by basaltic and tuffaceous layers in boreholes N, P, and Q (Figs. 7, 8, 12).

4.3 R3 system

The R3 system in central Taiwan comprises sandstone reservoirs in the Peiliao and Shiti Fm, with the Talu Sh serving as the caprock. The stratigraphic ages span the early to middle Miocene (Fig. 2). Borehole O (Fig. 6) represents vertical lithological variations within the R3 system in the onshore southern TB (Fig. 1).

The R3 system has up to 230 m of sandstone or intercalated sandstone/shale units, with a caprock of approximately 70 m thick shale at the top, as shown in borehole O (Fig. 6). The Talu Sh is about 70 m thick shale with a 10 m thick interbedded sandstone and shale. The top of the Peiliao Fm, acting as a secondary reservoir, consists of a fossiliferous/calcareous sandstone bed about 10 m thick, laterally equivalent to a limestone unit (Orbitoid Limestone, Chi 1981). The primary reservoir in the R3 system is a sandstone bed up to 50 m thick, directly underlying the calcareous sandstone unit. The lower section of the Peiliao Fm is primarily composed of interbedded sandstone and shale, with a thickness of about 65 m. In the middle of this section, a 15 m-thick shale layer is located (Fig. 6). The second reservoir unit of the R3 system is the Shiti Fm, which is divided into two units. The upper unit is dominated by interbedded sandstone/

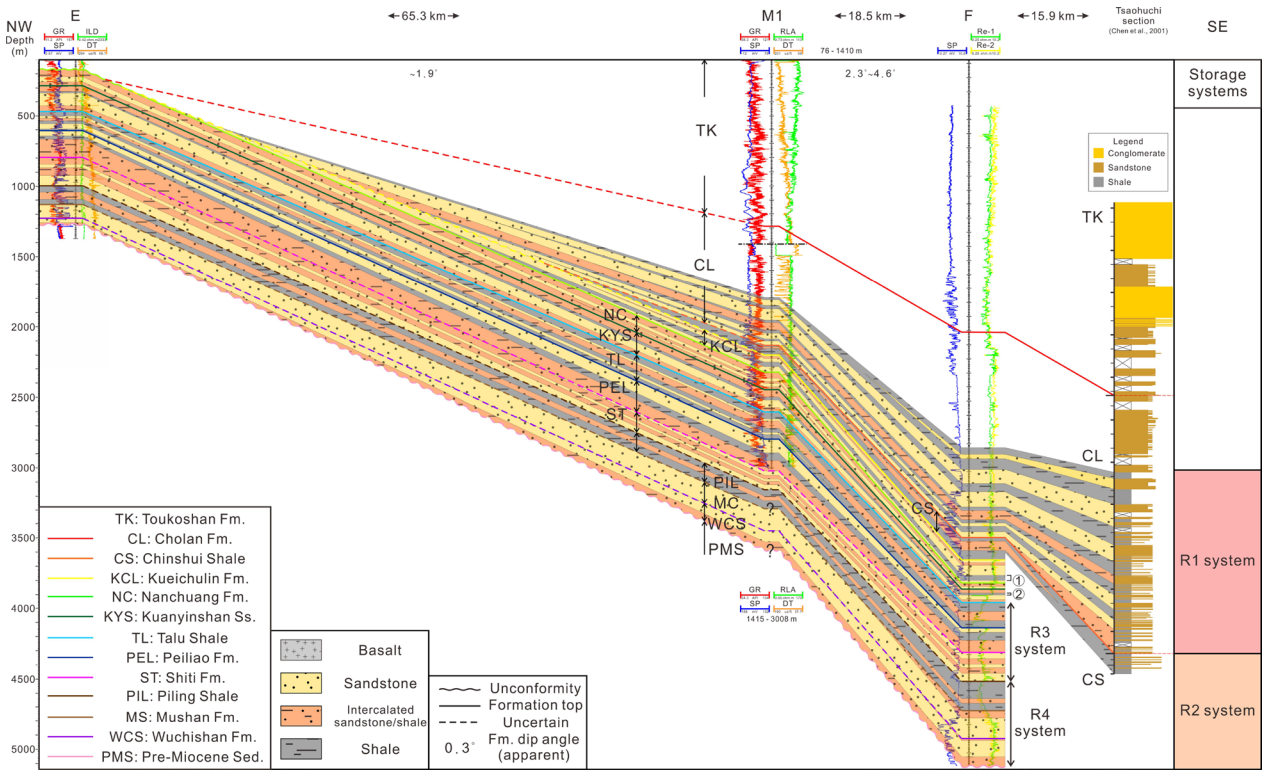

Fig. 10 Borehole stratigraphic correlation panel, Line-4, across the onshore and offshore NW–SE direction (see Fig. 1 for locations)

shale and sandstone, with a thickness of about 80 m. The lower unit comprises 65 m thick sandstone beds, with 10 m thick shale and intercalated sandstone/shale layers (Fig. 6).

According to the correlation panels, the R3 system exhibits excellent conditions for CO_2 storage, except for the southwest offshore area (shallower than 800 m) and the northeast corner of the study area (deeper than 3,500 m). For the north-to-south correlation panels (Figs. 7 and 8), the top and basal depths of the R3 system range from 470 to 3465 m (top) and 785 to 4000 m (base), respectively. The system includes 200–580 m thick reservoirs and a 75–560 m thick caprock, the thickest seal rock in the study area. For the west-to-east correlation panels (Figs. 9, 10, 11 and 12), the top and basal depths range from 470 to 4035 m (top) and 785 to 4520 m (base), respectively. The system also comprises 45–560 m thick seal rocks and 195–580 m thick reservoirs.

A moderately thick shale layer (15–60 m thick) in the middle of the Peiliao Formation serves as an intraformational seal, which is widely distributed and found in several boreholes. South of borehole L (Fig. 7), part of the R3 system is shallower than 800 m in the offshore area and unsuitable for CO_2 storage. Near borehole E (Fig. 10), the R3 system is buried at depths shallower than 800 m; however, this area is more than 60 km from the shoreline. North of borehole M1 (Fig. 8), part of the R3 system lies at depths greater than 3,500 m and has not been thoroughly penetrated by drilling (e.g., boreholes C and D) (Fig. 9).

4.4 R4 system

The R4 system, central Taiwan's deepest storage system, features thick sandstone layers in the Mushan and Wuchishan Formations, capped by the Piling Sh. Borehole I (Fig. 6) illustrates the vertical lithological variations of the R4 system in the onshore central-southern TB (Fig. 1). This system's age ranges from the late Oligocene to the early Miocene.

Overall, the R4 system includes sandstone beds up to 370 m thick, capped by approximately 115 m of shale, as shown in borehole I (Fig. 6). The Piling Sh is about 115 m thick, including a 20 m interbedded sandstone and shale unit. The upper reservoir of the R4 system features a sandstone bed from the Mushan Fm, divided into two sections. The upper section includes interbedded sandstone/shale and sandstone beds, approximately 65 m thick. In some areas, a Molluscan Limestone bed is at the Mushan Fm and Piling Sh boundary (Chi 1981). The lower section of the Mushan Fm consists of 70 m thick sandstone with intercalated sandstone/shale beds (Fig. 6).

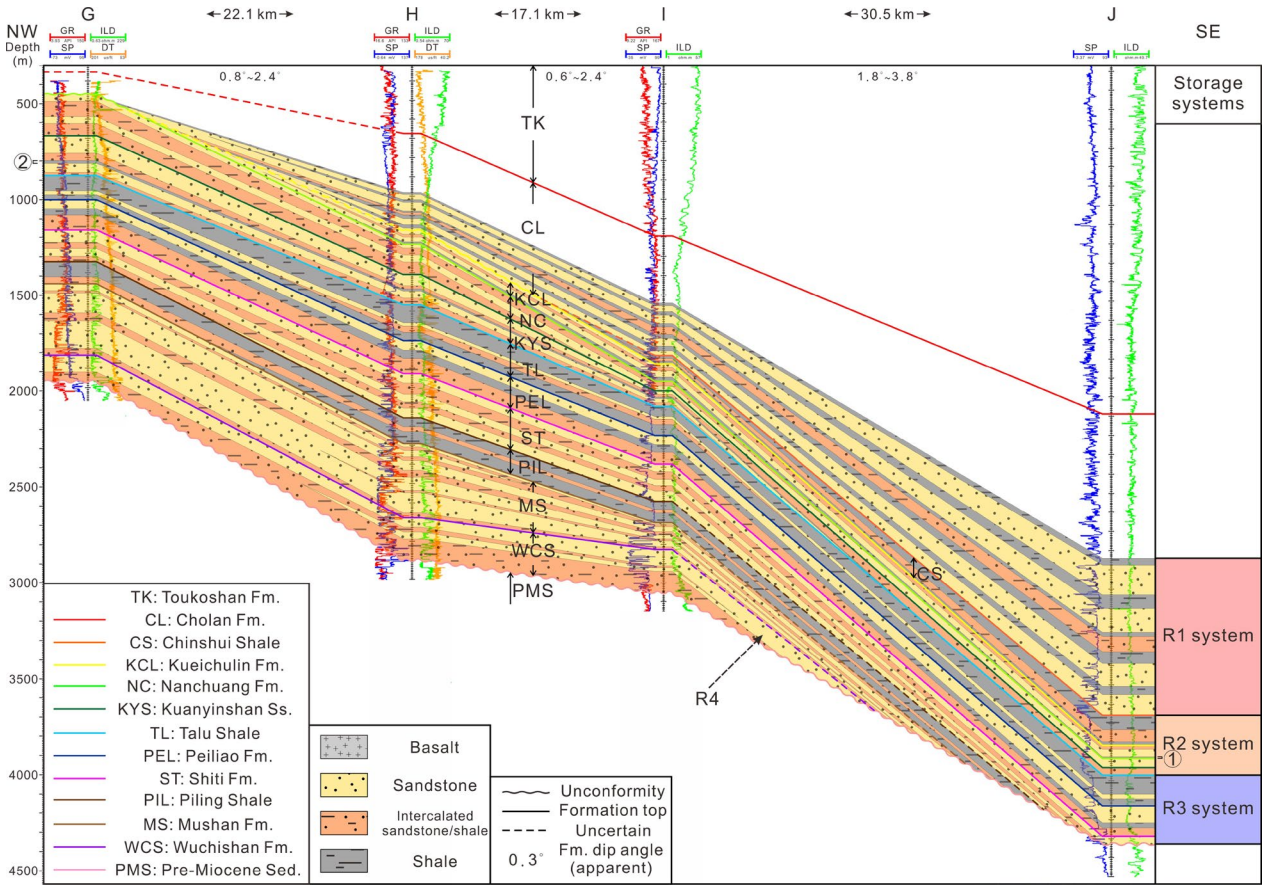

Fig. 11 Borehole stratigraphic correlation panel, Line-5, across the onshore and offshore NW–SE direction (see Fig. 1 for locations)

The lower reservoir features a 230 m thick sandstone bed from the Wuchishan Formation, the oldest exposed in the central Western Foothills. Pre-Miocene sediments resting below. The upper Wuchishan section has 115 m of sandstone mixed with sandstone/shale beds, each about 10 m thick. The lower section consists of interbedded sandstone and shale, around 115 m thick.

As the deepest storage system, the R4 system has not been entirely penetrated by drilling in the northeastern or eastern regions of the study area. Therefore, the depths in these regions are extrapolated from nearby boreholes. The uppermost part of the R4 system in the study area is deeper than 800 m, making it suitable for CO_2 storage. However, in the northeastern and eastern regions, where the depth exceeds 3500 m, CO_2 storage is not feasible. According to the correlation panels, the R4 system provides suitable conditions for CO_2 storage, except for the northeastern and eastern areas, where the depth exceeds 3500 m.

In the north–south correlation panels (Figs. 7 and 8), the R4 system's top and basal depths range from 785 to over 4000 m and 920 to over 4000 m, respectively. It comprises caprock 70–145 m thick and reservoirs 0–605 m thick, which are thin towards the south. The Wuchishan Formation disappears at boreholes N and O, while the Mushan Formation vanishes near borehole O (Figs. 7 and 8). In the west-to-east correlation panels (Figs. 9–12), the R4 system's top and bottom depths vary from 785 to 4520 m (top) and 920 to over 5125 m (base). This system includes seal rock with thicknesses ranging from 70 to 210 m and reservoirs 25 to 710 m thick.

4.5 Offshore seismic profiles

Five offshore seismic profiles are used to show the spatial variations in the studied formations and their correlations among the boreholes (Figs. 13 and 14). We convert the well logs of borehole K in the depth domain to the time domain using the time-depth chart from the vertical seismic survey of borehole K. We correlate the formation tops from borehole K to the MCS928-1a seismic profile (Fig. 13a). The formation tops from MCS928-1a are then correlated with other seismic profiles (Figs. 13 and 14). The seismic profiles show that the strata in the study area are mostly unaffected by faulting (Figs. 13 and 14). The

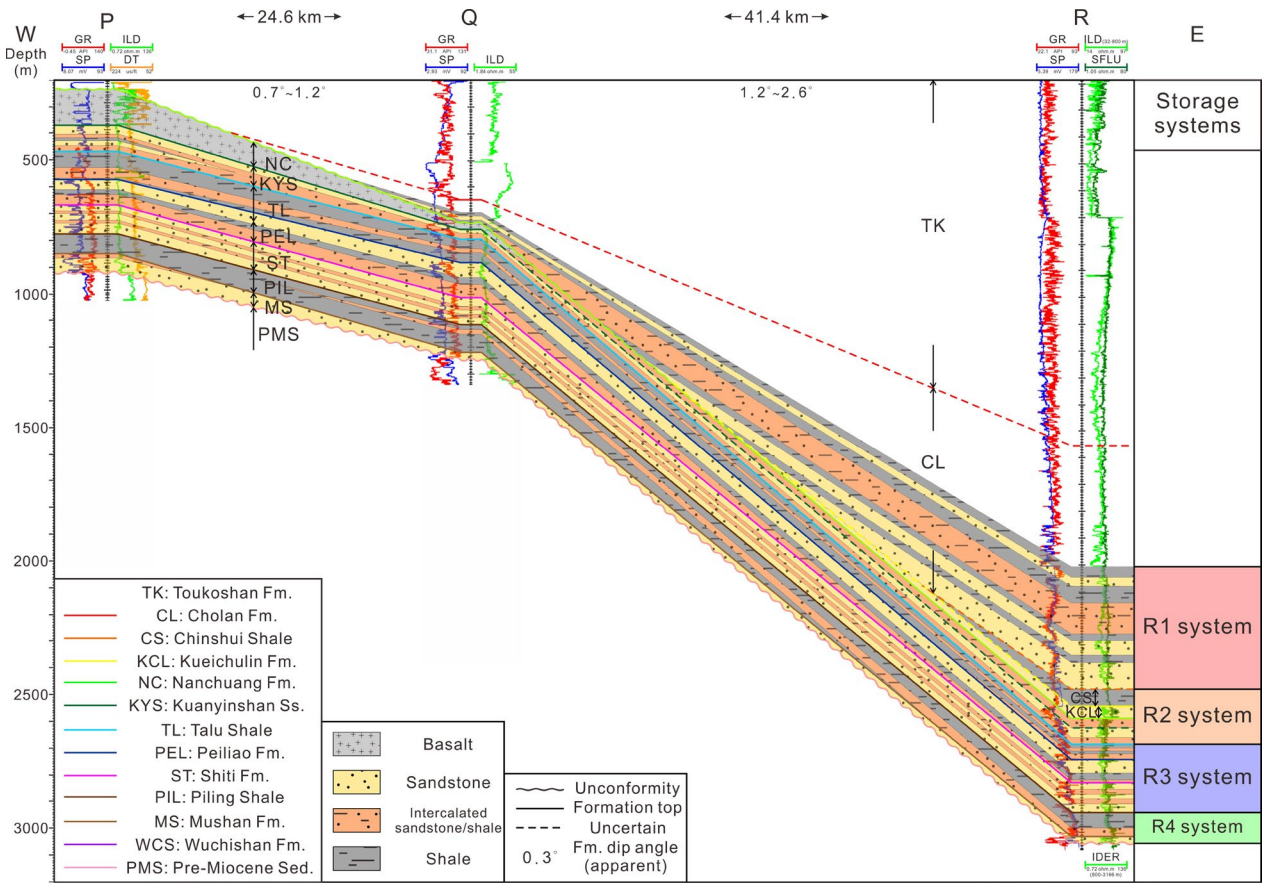

Fig. 12 Borehole stratigraphic correlation panel, Line-6, across the onshore and offshore NW–SE direction (see Fig. 1 for locations). Acronyms for well logs are SFLU: Spherically focused resistivity log. IDER: resistivity log

locations of the overlapping features seen in the seismic profiles are consistent with the positions shown on the borehole correlation panels (Figs. 7, 11, 13, and 14). The spatial thickness distribution of the formations is consistent with the borehole correlation panels and seismic profiles. The deposits of TB thin toward the south and west. The R1 disappears near boreholes G and N (Figs. 7, 11, 13 and 14). The Chinshui Sh disappears near the borehole H. The Kueichulin Fm disappears near boreholes G and N. The R3, R4, and lower part of R2 (Nanchuang Fm and Kuanyinshan Ss) show a uniform thickness and exhibit shallowing and thinning features toward the south (Fig. 13) and west (Fig. 14) from the basin center in the Taichung-Miaoli region. The Wuchishan Fm disappears in the south of the study area (Figs. 13b, 14b, and c), it is also shown in correlation panels (Figs. 7 and 11).

5 Porosity and permeability of potential CO_2 reservoirs

The porosity and permeability values shown in Fig. 15 were measured from core samples of sandstones and shaly sandstones from nine boreholes (i.e., boreholes D, F, F2, I, J, M1, S, T, and U) (Hsieh 1962; Hsu et al. 1969; Yang et al. 1969; Yang et al. 1971; Chan et al. 1974; Hsieh et al. 1974; Chan et al. 1978; Hsu et al. 1969; Sinotech Engineering Consultants, Inc., 2014; Yang 2015 and Lin 2018). These values of these major sandstone and shaly sandstone reservoirs are used to characterize the R1 to R4 systems.

5.1 Porosity

The nominal porosity of sandstones is better than the shaly sandstones (Fig. 16a, Table 2). Among the four systems, the R1 reservoirs show the highest average porosity values (29% for sandstones and 23% for shaly sandstones), and the R3 reservoir porosity readings are the lowest (20% for sandstones and 15% for shaly sandstones; Fig. 16a, Table 2). The average porosity values for the R2 reservoirs are 26% for sandstone and 20% for shaly sandstone, whereas the average porosity values for the R4 are 23% for sandstone and 17% for shaly sandstone.

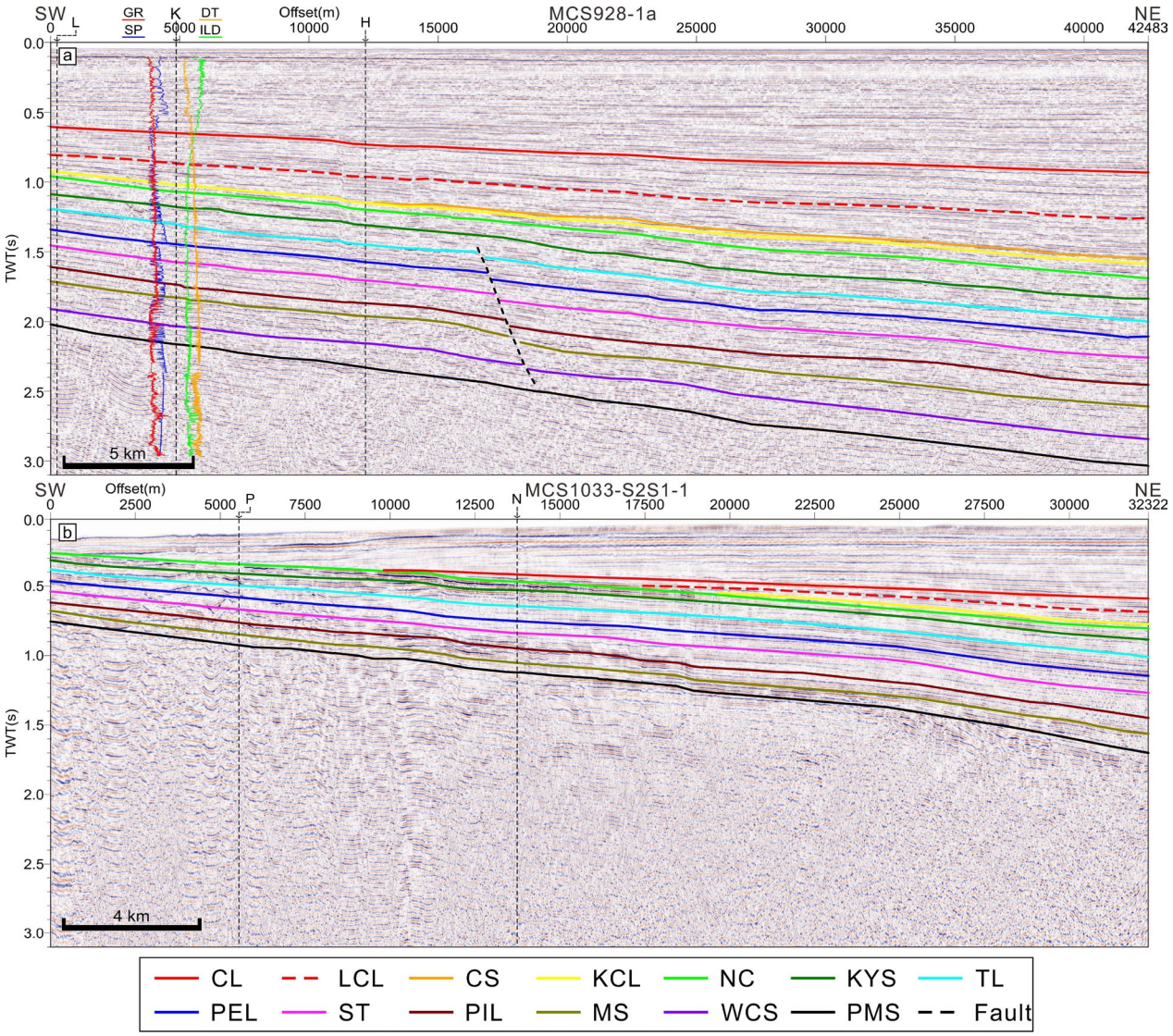

Fig. 13 Offshore seismic profiles in NE-SW direction: **a** MCS928-1a. **b** MCS1033-S2S1-1. Formation tops are correlated from borehole K as shown in (**a**). Projected locations of boreholes along the seismic profiles are also marked. Acronym for lower Cholan Formation is LCL

5.2 Permeability

The overall permeability of the shaly sandstone is not as good as that of sandstone. The averaged permeability of shaly sandstone is up to 18.3–170 mD (Table 2), which is considered as a good CO_2 reservoir ($\geq$ 20 mD as defined by Bachu et al. 2009). The average permeability of all four systems for sandstone is 243–1068 mD, which was relatively high and is considered as very good to excellent CO_2 storage reservoir. The permeability of most of the samples is greater than 20 mD for porosity around 15–40% (Fig. 17). The porosity/permeability of the sandstones shows a more clustered trend than that of the shaly sandstones. In summary, the porosity and permeability of the reservoir for CO_2 storage in the TB shows good CO_2 storage potential.

The average permeability of R3 reservoirs is the highest among the four systems (1068 mD for sandstone and 55.7 mD for shaly sandstone), in contrast to the lowest average porosity (Fig. 16b and Table 2). The average permeability values for the R1 reservoirs are 671 mD for sandstone and 170 mD for shaly sandstone; the R2 reservoirs average 586 mD for sandstones and 32.1 mD for shaly sandstone; and the R4 reservoirs average 243 mD for sandstones and 18.3 mD for shaly sandstone.

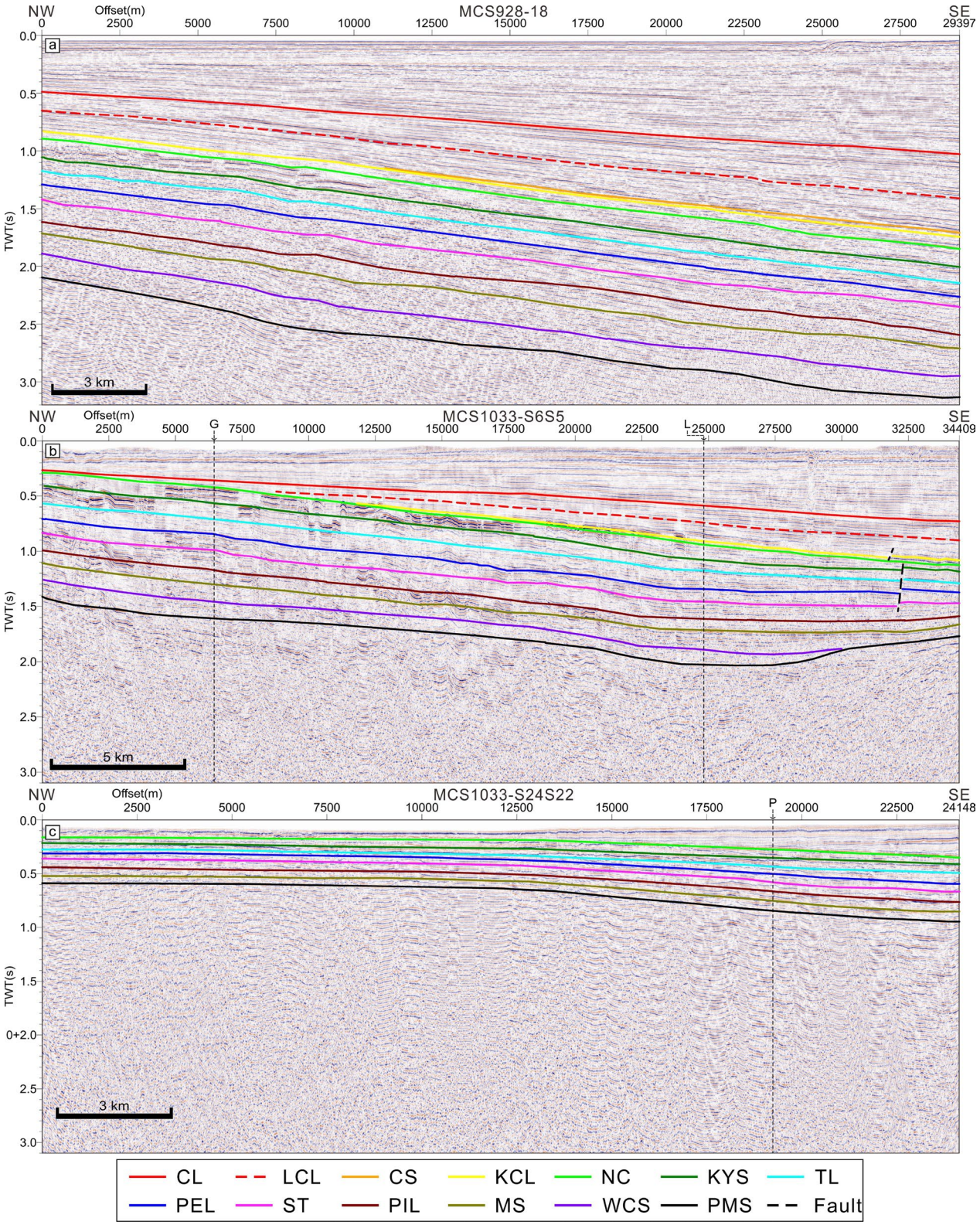

Fig. 14 Offshore seismic profiles in NW–SE direction: **a** MCS928-18. **b** MCS1033-S6S5. **c** MCS1033-S24S22. Formation tops are correlated from borehole K as shown in Fig. 13a. Projected locations of boreholes along the seismic profiles are also marked. Acronym for lower Cholan Formation is LCL

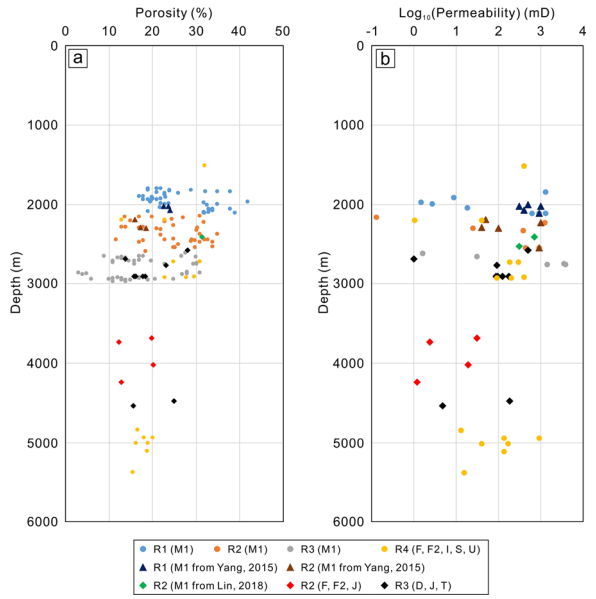

Fig. 15 **a** A plot of porosity values versus depth from borehole core samples for sandstones and shaly sandstones of R1, R2, R3, and R4 systems. **b** A plot of permeability values versus depth from borehole core samples for sandstones and shaly sandstones of R1, R2, R3, and R4 systems. Samples from the M1 well are from Sinotech Engineering Consultants, Inc, (2014) with a few samples from Yang (2015) and Lin (2018). The R1 system of the M1 well from Sinotech Engineering Consultants, Inc, (2014) and Yang (2015) are infilled blue circles and dark blue triangles, respectively. The R2 system of the M1 well from Sinotech Engineering Consultants, Inc, (2014), Yang (2015), Lin (2018), and the R2 system of F, F2, J wells are infilled orange circles, dark orange triangles, green diamonds and red diamonds, respectively. The R3 system of the M1 well from Sinotech Engineering Consultants, Inc, (2014) and the R3 system of D, J, T wells are infilled grey circles and black diamonds, respectively. The R4 system of F, F2, I, S, U wells are infilled yellow circles

6 Discussion

This section focuses on central Taiwan's three primary CO_2 emission sources: the TPP, CCIP, and MTIP. Considering the maximum migration distance of the injected CO_2 plume (Birkholzer et al. 2015; Williams and Chadwick 2021; Rathmaier et al. 2024), the square area of the potential injection site with the TPP, CCIP, or MTIP at the center is 20 km by 20 km. The R1–4 storage systems at these sites are evaluated regarding the spatial distribution of the caprock thickness, reservoir thickness, and depth ranges. In addition, the porosity and permeability of the reservoir rocks are assessed quantitatively. Tables 3, 4 and 5 list the storage system parameters for the TPP, CCIP, and MTIP sites.

The TPP and CCIP sites are located in the center of the TB and their storage system characteristics shows thick caprock/reservoir pairs. Most of the R4 and lower R3 systems are unsuitable as CO_2 reservoirs because their burial depths are greater than 3500 m. The MTIP site is located on the southern margin of the basin. Its storage systems (R1, R3, and R4) lie within a suitable depth range of 800–3500 m; however, its reservoir thickness is generally thinner than that in the basin center. Our results provide a holistic understanding of carbon storage systems in central and offshore Taiwan and directions for selecting suitable carbon storage systems in the areas of interest.

6.1 Taichung coal-fired power plant (TPP)

Boreholes B, C, D, M1, and F represent the TPP at the northern coast of the study area as references (Fig. 1). These boreholes and borehole correlation panels (Lines 1–4; Figs. 7, 8, 9 and 10) serve as the basis for our discussion. Table 3 summarises the storage system parameters of the TPP sites.

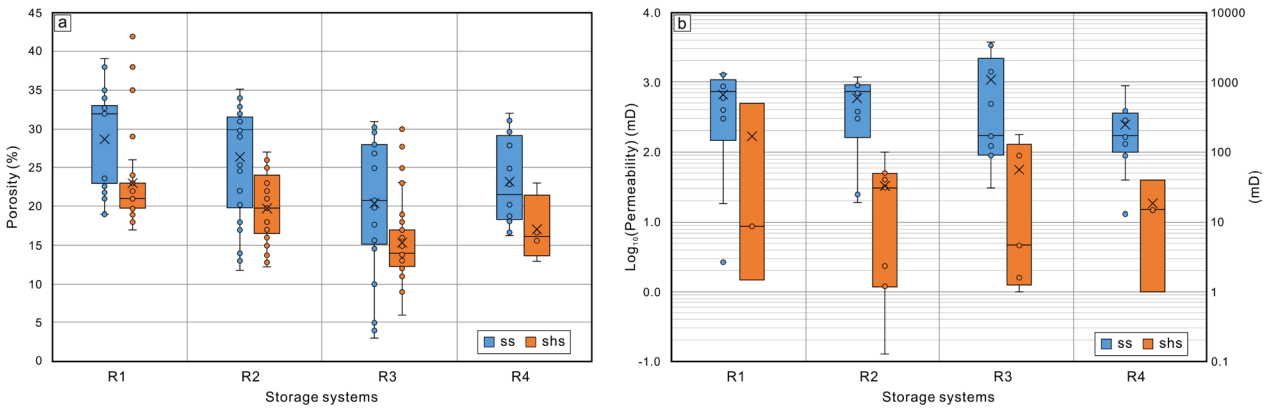

Fig. 16 A plot showing the ranges of measured porosity and permeability for sandstones (ss) and shaly sandstone (shs) of the R1, R2, R3, and R4 systems. **a** the range of porosity for R1 to R4 systems (**b**) the range of permeability for R1 to R4 systems. Blue and orange colors are sandstones (ss) and shaly sandstone (shs), respectively. Note that the averaged values of permeability are log-scale averages

Table 2 A list of measured porosity and permeability values from core sample

System	Porosity-ss			Porosity-shs		
	Min	Mean	Max	Min	Mean	Max
R1	0.19	0.29	0.39	0.17	0.23	0.42
R2	0.12	0.26	0.35	0.14	0.20	0.27
R3	0.03	0.20	0.31	0.06	0.15	0.30
R4	0.16	0.23	0.32	0.13	0.17	0.23
System	**Permeability-ss (mD)**			**Permeability-shs (mD)**		
	Min	**Mean**	**Max**	**Min**	**Mean**	**Max**
R1	3	671	1300	1.5	170	500
R2	19	586	1200	0.1	32.1	100
R3	31	1068	3800	1	55.7	180
R4	13	243	890	1	18.3	39

It shows the maximum, mean, and minimum of porosity and permeability for R1 ~ R4 systems. Porosity and permeability are only considered for sandstones and shaly sandstones. Acronyms for the lithology are ss: sandstone, and shs: shaly sandstone. Note that the mean values of permeability are log-scale averages

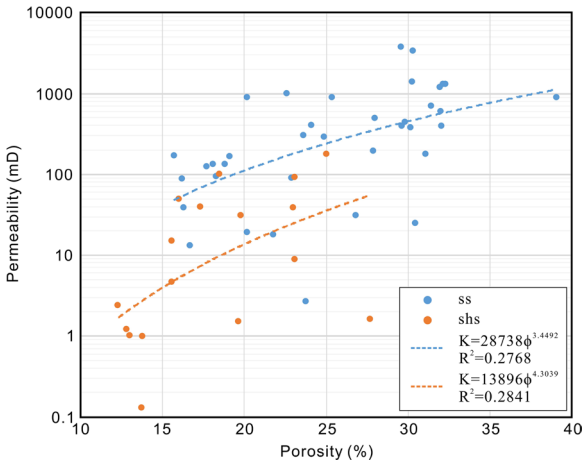

Fig. 17 A plot shows the porosity–permeability relationship of sandstone and shaly sandstone. Blue and orange circles are sandstone (ss) and shaly sandstone (shs) samples, respectively. Blue and orange dotted lines are the porosity–permeability relationship of sandstone and shaly sandstone, respectively

(1) R1 system: The R1 system exhibits good conditions at the TPP site regarding suitable depth range and seal/reservoir-rock pairs. The top of the R1 system at the TPP site is 1,450 to 2600 m deep (Table 3, R1). The R1 system (lower Cholan Fm) is composed of 5–6 subsystems with 10–60 m thick seal rocks and 30–90 m thick reservoirs.

(2) R2 system: The top of the R2 system at the TPP site is approximately 1900–3200 m (Table 3, R2), with 70–160 m thick seal rock and 300–900 m reservoirs. Two thin shale layers may also serve as intraformational seals, with an approximately 30 m thick upper intra-seal and an approximately 20 m thick lower intra-seal.

(3) R3 system: The top of the R3 system at the TPP site is 2750 to 3700 m deep (Table 3, R3). Although part of the R3 system is deeper than 3500 m in the northeast corner of the TPP site, it shows suitable conditions for CO_2 storage in the rest of the area. Another advantage of the R3 system is the thicker caprocks and reservoirs. The caprock, Talu Sh, is approximately 180–560 m thick, and the reservoir is thicker than 400 m. A 30–60 m thick intraformational shale is present within the middle Peiliao Fm. This shale bed divided the R3 system into two substorage systems.

Table 3 List of properties of carbon storage systems in and around the Taichung Power Plant (TPP) site

Systems	Caprock thickness	Reservoir thickness	Depth of top system
R1	10 – 60 m (5 – 6 layers)	30 – 90 m (5 – 6 layers)	1450 – 2600 m
R2	70 – 160 m	300 – 900 m	1900 – 3200 m
R3	180 – 560 m	400 – 450 m (estimated)	2750 – 3700 m
R4	120 – 150 m (estimated)	370 – 610 m (estimated)	3700 – 4500 m

TPP is in the middle of a 20 km × 20 km square. The R3 and R4 systems lie too deep in this region and are not drilled by any boreholes within this assessed site. The caprock/reservoir thicknesses and depths for R3 and R4 systems are interpolated from nearby boreholes. The values are marked as estimated

Table 4 A list of properties of carbon storage systems in and around the Changhua Coastal Industrial Park (CCIP) site

Systems	Caprock thickness	Reservoir thickness	Depth of Top
R1	10 – 25 m (5 layers)	25 – 80 m (5 layers)	1385 – 2400 m
R2	35 – 115 m	280 – 505 m	1655 – 2850 m
R3	150 – 240 m	240 – 400 m (estimated)	2085 – 3320 m
R4	> 100 m (estimated)	350 – 600 m (estimated)	2800 – 4350 m (estimated)

The M1 well is in the middle of a 20 km × 20 km square. Because the lower R3 system and the R4 system lie too deep in this region and they are not drilled by any boreholes within this assessed site. The caprock/reservoir thicknesses and depths for R3 and R4 systems are interpolated from nearby boreholes. The values are marked as estimated

Table 5 A list of properties of carbon storage systems in and around the Mailiao Taisu Industrial Park (MTIP) site

Systems	Caprock thickness	Reservoir thickness	Depth of Top
R1	10 – 20 m (3 – 4 layers)	10 – 45 m (3 – 4 layers)	650 – 1300 m
R2	0 – 35 m	50 – 300 m	680 – 1515 m
R3	85 – 170 m	210 – 370 m	825 – 1735 m
R4	110 – 140 m	0 – 545 m	1160 – 2180 m

The MTIP is in the middle of a 20 km × 20 km square. Formations of the Chinshui Shale, Mushan Formation, and Wuchishan Formation are missing in some areas around the MTIP site; thus, the minimum thickness is marked by 0

(4) R4 system: Although the R4 system has thick reservoirs (> 370 m) and caprocks (> 120 m), the R4 system is not suitable for CO_2 storage because its depth is greater than 3500 m. The top of the R4 system at the TPP site is approximately 3700–4500 m deep (Table 3, R4), deeper than 3500 m. As the R4 system is not penetrated by drilling, we estimate the thicknesses of the caprock and reservoirs in the ranges of 120–150 m and 370–610 m, respectively, by interpolation from nearby borehole data.

6.2 Changhua coastal industrial park

The CCIP is located in the central part of the study area on the reclaimed coastal land in Changhua County. We present the data in Table 4 using nearby boreholes M1, H, I, F, and C (Fig. 1) and borehole correlation panels (Lines 1, 2, 4, 5; Figs. 7, 8, 10, and 11) as references.

(1) R1 system: Similar to the TPP site, the R1 system shows good conditions at the CCIP site regarding a suitable depth range and seal/reservoir-rock pairs. The top of the R1 system at the CCIP site is 1385 to 2400 m in depth (Table 4, R1). The R1 system is composed of five subsystems with 10–25 m thick seal rocks and a 25–80 m thick reservoir.
(2) R2 system: The top of the R2 system at the CCIP site is approximately 1655–2850 m in depth (Table 4, R2), with 35–115 m thick seal rock and 280–505 m thick reservoirs. Two thin shale layers that may also serve as intraformational seals: a 20–30 m thick upper intra-seal and a 10–20 m thick lower intra-seal. Line-4 (Fig. 10) indicates that the Chinshui Sh caprock has disappeared approximately 23 km from the central point (M1 well) of the CCIP site.
(3) R3 system: The top of the R3 system at the CCIP site is 2085 to 3320 m in depth (Table 4, R3). We estimate that the caprock is approximately 150–240 m thick, and the range of the reservoir is 240–400 m. A 30–55 m thick intraformational shale is present within the middle part of the Peiliao Fm.
(4) R4 system: Good conditions are observed at the southern CCIP site with a thick caprock/reservoir and depth distribution (< 3500 m) (Figs. 1 and 8). The top of the R4 system at the CCIP site is approximately 2800–4350 m in depth (Tables 4 and R4). The thicknesses of the caprock and reservoir are estimated to exceed 100 m and 350–600 m, respectively. The R4 system at the northern CCIP site is more than 3500 m deep, making it unsuitable for CO_2 storage.

6.3 Mailiao Taisu industrial park

Boreholes K, L, I, N, O, and Q represent Mailiao Taisu Industrial Park in the southern study area of Yunlin County as references (Fig. 1). These boreholes and borehole correlation panels (Lines 1, 2, 5, and 6; Figs. 7, 8, 11, and 12) serve as the basis for our discussion.

(1) R1 system: Except for the southwest of the MTIP site, which is extremely shallow (< 800 m), the R1 system shows good conditions for storing CO2 regarding suitable depth distribution and seal/reservoir-rock pairs. The top of the R1 system at the MTIP site is 650 to 1300 m in depth (Table 5, R1) and consists of 3–4 subsystems with 10–20 m thick seal rock and 10–40 m thick reservoirs.
(2) R2 system: Although most of the R2 system is within suitable conditions, including the depth

range and thick reservoirs, it lacks regional sealed rock. The top of the R2 systems at the MTIP site is approximately 680–1,515 m in depth (Table 5, R2), with 0–35 m thick seal rock and 50–300 m thick reservoirs. The Nanchuang Fm is missing in some places and is replaced by basaltic/tuffaceous layers near the N, P, and O wells. It is also an unsuitable reservoir rock for CO_2 storage.

(3) R3 system: The top of the R3 system at the MTIP site is 825 to 1735 m in depth (Table 5, R3), with a 90–170 m thick seal rock layer and a 210–370 m thick reservoir. A thin shale layer 10–25 m in thickness may also serve as an intraformational seal.

(4) R4 system: The R4 system shows good potential for storing CO_2, except near borehole O at the south of the MTIP site. The top of the R4 system at the MTIP site is approximately 1160–2180 m in depth (Table 5, R4) and is composed of a 110–140 m-thick caprock and a 0–545 m-thick reservoir. Line-2 (Fig. 8) shows that the Wuchishan Fm thins and disappears at the northeast MTIP site. The Mushan Fm also thins and disappears near borehole O at the southern MTIP site (Fig. 8).

7 Conclusions

This study used 22 borehole data to identify suitable stratigraphic trap systems for carbon storage in central Taiwan. It established a solid base for estimating carbon storage capacity and performing post-injection simulations. We employed borehole data to characterize the geological parameters (e.g., spatial distribution of depths, thicknesses of reservoirs and caprocks, and porosity and permeability of reservoirs) for CO_2 storage in central Taiwan and offshore areas. In descending order, the carbon storage systems identified include the R1, R2, R3, and R4 systems.

The carbon storage systems in the center of TB feature thick reservoirs and caprocks; however, the R4 and lower R3 systems are too deep (> 3500 m) to store CO_2 effectively. In contrast, the storage systems along the southern basin margin in central Taiwan are situated at a suitable depth range (i.e., between 800 and 3500 m). Nevertheless, their reservoirs are generally thinner than those of the basin center. The carbon storage systems at three sites (TPP, CCIP, and MTIP), which are significant sources of stationary CO_2, are examined in detail:

(1) TPP site: The R2 system features the best criteria for depth and thickness distribution of caprock-and-reservoir pairs. The R1 system shows good conditions owing to its suitable depth range and seal/reservoir-rock pairs. Although the R3 system is deeper than 3500 m in the northeastern corner of the TPP site, it exhibits favorable conditions for CO_2 storage in the study area.

(2) CCIP site: Similar to the TPP site, the R2 system shows the best potential among all systems. The R1 and R3 systems also exhibit favorable conditions for CO_2 storage. The R4 system is only suitable for carbon storage at the southern CCIP site.

(3) MTIP site: The R3 system is the most effective for carbon storage, considering the depth and thickness of the seal-and-reservoir pairs. The R1 and R4 systems showed limited conditions for CO_2 storage, while the R2 system was unsuitable.

The porosity and permeability of reservoirs measured from borehole cores shows that the average porosities for R1 to R4 systems are in the ranges of 20–39% for sandstones and 16–23% for shaly sandstones, respectively. The average permeabilities for R1 to R4 systems were in the ranges of 243–1068 mD for sandstones and 18.3–170 mD for shaly sandstones, respectively. The measured reservoir porosity and permeability shows very good-to-excellent CO_2 storage potential in the study area.

Acknowledgements

This study was funded by the National Science and Technology Council (NSTC) of Taiwan under grant MOST 105-3113-E-008-009. This NSTC-funded joint study is a collaborative work between universities, the CPC Corporation, and the Taiwan Power Company. We thank Drs. Chih-Cheng Yang and Chien-Ping Lee for their suggestions and assistance during period of conducting research. We thank the reviewers for their thoughtful comments, which have greatly improved the quality of this manuscript.

Authors' contribution

Wei-Di Syu: Writing – original draft, Visualization, Methodology, Formal analysis, Data curation. Andrew Tien-Shun Lin: Writing – review & editing, Supervision, Software, Resources, Funding acquisition, Conceptualization. Chi-Wen Yu: Supervision, Resources, Funding acquisition. Jia-Jyun Dong: Methodology, Resources acquisition. Ming-Wei Yang: Resources acquisition. Chung Huang: Resources acquisition. Shu-Kun Hsu: Resources acquisition.

Data availability

Some porosity or permeability data supporting the findings of this study are available in the articles (Sinotech Engineering Consultants, Inc. 2014; Yang 2015; Lin 2018).

Declarations

Competing interests

The authors declare that there is no financial/personal interest or belief that could affect the objectivity of this manuscript.

Received: 1 February 2024 Accepted: 4 March 2025
Published online: 25 April 2025

References

Anwar MN, Fayyaz A, Sohail NF, Khokhar MF, Baqar M, Khan WD, Rasool K, Rehan M, Nizami AS (2018) CO_2 capture and storage: a way forward for

sustainable environment. J Environ Manage 226:131–144. https://doi.org/10.1016/j.jenvman.2018.08.009
Bachu S, Hawkes C, Lawton D, Pooladi-Darvish M, Perkins E (2009) CCS Site Characterization Criteria. Technical Study Report no. 2009/10, IEA Greenhouse Gas R and D Programme, 112 pp.
Birkholzer JT, Oldenburg CM, Zhou Q (2015) CO_2 migration and pressure evolution in deep saline aquifers. Int J Greenhouse Gas Control 40:203–220. https://doi.org/10.1016/j.ijggc.2015.03.022
Brantley D, Shafer J, Lakshmi V (2015) CO_2 injection simulation into the South Georgia Rift Basin for geologic storage: a preliminary assessment. Environ Geosci 22(1):1–18. https://doi.org/10.1306/eg.09191414008
Central Geological Survey, 1986. General Geologic Map of Taiwan. Central Geological Survey, MOEA.
Chadwick A, Arts R, Bernstone C, May F, Thibeau S, Zweigel P (2008) Best Practice for The Storage of CO_2 in Saline Aquifers-Observations and Guidelines from The SACS and CO_2STORE projects, British Geological Survey Occasional Publication 14, 267 pp.
Chan Y-K, Liu K-H (1974) Subsurface geological report of the T wildcat. CPC Corporation, Chiayi, p 29
Chan Y-K, Liu C-T, Fan K-W (1978) Subsurface geological report of the I well, Lukang field. CPC Corporation, Changhua, p 38
Chang Y-L, Cheng K-H (1978) Subsurface geological report of the Q well, Taishi. CPC Corporation, Yunlin, p 32
Chen W-S (2016) An introduction to the geology of Taiwan. Geol Soc Taiwan. https://doi.org/10.1016/j.margeo.2015.11.010
Chen W-S, Ridgway KD, Horng C-S, Chen Y-G, Shea K-S, Yeh M-G (2001) Stratigraphic architecture, magnetostratigraphy, and incised-valley systems of the Pliocene-Pleistocene collisional marine foreland basin of Taiwan. Geol Soc Am Bull 113(10):1249–1271. https://doi.org/10.1130/0016-7606(2001)113%3c1249:SAMAIV%3e2.0.CO;2
Chi W-R (1981) The biohorizons of the Operculina Limestone, Orbitoid Limestone, and Molluscan Limestone in the subsurface sediments from the Peikang-Yunlin area. Ti-Chih 3:63–71
Chiu T-H (2018) A study on paleoenvironments of the late pliocene to early pleistocene foreland basin in the Western Foothills of Central Taiwan. Department of Earth Sciences, National Central University, Taoyuan, p 95
Chou J-T (1974) A sedimentologic and paleogeographic study of the Miocene Wuchihshan formation in western Taiwan. Pet Geol Taiwan 11:41–55
Chou J-T (1976) A sedimentologic and paleogeographic study of the Miocene Shihti formation in western Taiwan. Pet Geol Taiwan 13:119–138
Daniel, R.F., Kaldi, J.G., 2008. Evaluating seal capacity of caprocks and intraformational barriers for the geosequestration of CO2, PESA Eastern Australia Basins Symposium III, 475-484
Hong E, Wang Y (1988) Basin analysis of the upper Miocene—lower pliocene series in Northwestern Taiwan. Ti-Chih 8:1–20
Hsieh S-H (1962) Subsurface geological report of the U well, Suan Tou. CPC Corporation, Chiayi, p 12
Hsieh SH (1968) Sandstone reservoirs in the lower Miocene Mushan formation in the Miaoli area Taiwan. Pet Geol Taiwan 6:139–156
Hsieh C-C, Huang T-C (1974) Subsurface geological report of the D well, Hou-Li Structure. CPC Corporation, Taichung, p 17
Hsieh B-Z, Nghiem L, Shen C-H, Lin Z-S (2013) Effects of complex sandstone–shale sequences of a storage formation on the risk of CO_2 leakage: case study from Taiwan. Int J Greenhouse Gas Control 17:376–387. https://doi.org/10.1016/j.ijggc.2013.05.030
Hsieh AI, Vaucher R, Löwemark L, Dashtgard SE, Horng CS, Lin AT, Zeeden C (2023) Influence of a rapidly uplifting orogen on the preservation of climate oscillations. Paleoceanogr Paleoclimatol 38(6):e2022PA004586. https://doi.org/10.1029/2022PA004586
Hsu C-H, Liu C-T, Yang C-Y, Lin Y-F (1969) Subsurface geological report of the F2 well, Pakuashan anticline. CPC Corporation, Changhua, p 23
Hsu S-K, Lin AT, Wang C-Y, Yang K-M, Lin Z-S, Huang H-C, Li M-H, Hong J-H (2013) Research on CO2 Geosequestration in the Taiwan Area (II), Ministry of Science and Technology, Project Completion Report, 139 pp.
Hu J-C, Angelier J, Yu S-B (1997) An interpretation of the active deformation of southern Taiwan based on numerical simulation and GPS studies. Tectonophysics 274(1–3):145–169. https://doi.org/10.1016/S0040-1951(96)00302-2
Lin, A.T., 2001. Cenozoic Stratigraphy and Tectonic Development of the West Taiwan Basins. Doctoral dissertation, Department of Earth Sciences, University of Oxford, 245 pp.
Lin C-K (2008) Algorithm for determining optimum sequestration depth of CO_2 trapped by residual gas and solubility trapping mechanisms in a deep saline formation. Geofluids 8(4):333–343. https://doi.org/10.1111/j.1468-8123.2008.00221.x
Lin H-C (2018) Porosity and Permeability Variations with Depth Inferred from Porosity and Permeability Measurements on Cores. MSc. Thesis, Graduate Institute of Applied Geology, National Central University, 165 pp
Lin AT (2021b) A study on sequence stratigraphy and sedimentary environments in southwest Taiwan. CPC Corporation Project Completion Report, Kaohsiung City, p 80
Lin AT, Watts AB (2002) Origin of the West Taiwan basin by orogenic loading and flexure of a rifted continental margin. J Geophys Res Solid Earth. https://doi.org/10.1029/2001JB000669
Lin AT, Watts AB, Hesselbo SP (2003) Cenozoic stratigraphy and subsidence history of the South China Sea margin in the Taiwan region. Basin Res 15(4):453–478. https://doi.org/10.1046/j.1365-2117.2003.00215.x
Lin W, Yeh E-C, Ito H, Hirono T, Soh W, Wang C-Y, Ma K-F, Hung J-H, Song S-R (2007) Preliminary results of stress measurement using drill cores of TCDP Hole-A: an application of anelastic strain recovery method to three-dimensional in-situ stress determination. Terr Atmos Ocean Sci 18(2):379
Lin AT, Wang C-Y, Lin J-Y, Lin C-W, Yang K-M, Jean J-S, Huang H-C, Tien Y-M, Ni C-F, Lin Z-S, Hong J-H, Liou T-S, Hsieh B-Z (2014) Assessment of CO_2 Geological Storage in Taiwan and the Developments of Pilot Test Site and Integrated Technology for CO_2 Geosequestration(I), Ministry of Science and Technology, Project Completion Report, 213 pp.
Lin AT, Wang C-Y, Hsu S-K, Ni C-F, Yang K-M, Rau R-J, Hsieh B-Z (2016) Assessment on CO_2 Geological Storage in Deep Saline Formations of Taiwan and Development of Pilot Test Site for CO_2 Geosequestration. Ministry of Science and Technology, Project Completion Report, 224 pp.
Lin AT, Yang C-C, Wang M-H, Wu J-C (2021a) Oligocene-Miocene sequence stratigraphy in the northern margin of the South China Sea: an example from Taiwan. J Asian Earth Sci 213:104765. https://doi.org/10.1016/j.jseaes.2021.104765
Ma P, He J (2017) Research on model and related parameters of supercritical CO_2 injection into depleted reservoir. IOP Conf Ser Earth Environ Sci 78(1):012006. https://doi.org/10.1088/1755-1315/78/1/012006
NDC, 2022. 2022.03.30_Taiwan's Pathway to Net-Zero Emissions in 2050. National Development Council, Republic of China. https://www.ndc.gov.tw/en/Content_List.aspx?n=4F53FB476A3EC255.
Pan T-Y, Lin AT-S, Chi W-R (2015) Paleoenvironments of the evolving P liocene to early P leistocene foreland basin in northwestern T aiwan: an example from the D ahan R iver section. Island Arc 24(3):317–341. https://doi.org/10.1111/iar.12113
Rathmaier D, Naim F, William AC, Chakraborty D, Conwell C, Imhof M, Holmes GM, Zerpa LE (2024) A Reservoir modeling study for the evaluation of CO_2 storage upscaling at the decatur site in the Eastern Illinois Basin. Energies 17(5):1212. https://doi.org/10.3390/en17051212
Sasaki K, Fujii T, Niibori Y, Ito T, Hashida T (2008) Numerical simulation of supercritical CO_2 injection into subsurface rock masses. Energy Convers Manage 49(1):54–61. https://doi.org/10.1016/j.enconman.2007.05.015
Savaresi A (2016) The Paris agreement: a new beginning? J Energy Nat Resour Law 34(1):16–26. https://doi.org/10.1080/02646811.2016.1133983
Sinotech Engineering Consultants, Inc., (2014) Geological Investigation and Technology Development of a Pilot Test Site for Carbon Storage (Phase-1). Taiwan Power Company, Project Completion Report, 558 pp.
Span R, Wagner W (1996) A new equation of state for carbon dioxide covering the fluid region from the triple-point temperature to 1100 K at pressures up to 800 MPa. J Phys Chem Ref Data 25(6):1509–1596. https://doi.org/10.1063/1.555991
Tang C-H (1971) Stratigraphical relation of the Talu Shale to the Peiliao formation in northwest Taiwan. Pet Geol Taiwan 8:175–186
Tang C-H (1972) Depositional environment of the Miocene Talu sand reservoir, northwest Taiwan, and the possibilities of stratigraphic traps. Pet Geol Taiwan 10:109–121
Teng LS, Lin AT (2004) Cenozoic tectonics of the China continental margin: insights from Taiwan. Geol Soc 226(1):313–332. https://doi.org/10.1144/GSL.SP.2004.226.01.17
Williams GA, Chadwick RA (2021) Influence of reservoir-scale heterogeneities on the growth, evolution and migration of a CO_2 plume at the Sleipner Field, Norwegian North Sea. Int J Greenhouse Gas Control 106:103260. https://doi.org/10.1016/j.ijggc.2021.103260

Wu W-J, Dong J-J (2012) Determining the maximum overburden along thrust faults using a porosity versus effective confining pressure curve. Tectonophysics 578:63–75. https://doi.org/10.1016/j.tecto.2011.12.028
Wu K-H, Hsu C-H (1991) Subsurface geological report of the S wildcat, Shuilin structure. CPC Corporation, Yun-Lin, p 18
Yang C-Y, Huang T-C (1969) Subsurface geological report of the F well, Pakuashan anticline. CPC Corporation, Changhua, p 23
Yang C-Y, Huang T-C (1971) Subsurface Geological Report of the J well on the Tionchung culmination of the Pakuashan anticline. CPC Corporation, Changhua, p 24
Yang S-P (2015) Exploring the effect of lithology characters and tectonization on permeability and porosity of clastic sedimentary rocks by using deep-drilling cores. MSc. Thesis, Graduate Institute of Applied Geology, National Central University, 163 pp
Ye M-G, Yang J-H (1993) Subsurface geological report of the O well, lunfong structure Taihsi. CPC Corporation, Yunlin, p 22
Yu N-T, Teng LS, Chen W-S, Yue L-F, Chen M-M (2013) Early post-rift sequence stratigraphy of a Mid-Tertiary rift basin in Taiwan: insights into a siliciclastic fill-up wedge. Sed Geol 286:39–57. https://doi.org/10.1016/j.sedgeo.2012.12.009

Publisher's Note